Pose Stabilization of a Bar Tethered to Two Aerial Vehicles

Pedro O. Pereira and Dimos V. Dimarogonas

Abstract

This work focuses on the modeling, control and analysis of a bar, tethered to two unmanned aerial vehicles, which is required to stabilize around a desired pose. We follow a Newtonian approach when deriving the equations of motion, we close the loop by equipping each UAV with a PID control law, and finally we linearize the closed-loop vector field around some equilibrium points of interest. When requiring the bar to stay on the horizontal plane and under no normal stress, we verify that the bar's motion is decomposable into three decoupled motions, namely a longitudinal, a lateral and a vertical: for a symmetric system, each of those motions is further decomposed into two decoupled sub-motions, one linear and one angular; for an asymmetric system, we provide relations on the UAVs' gains that compensate for the system asymmetries and which decouple the linear sub-motions from the angular sub-motions. From this analysis, we provide conditions, based on the system's physical parameters, that describe *good* and *bad* types of asymmetries. Finally, when requiring the bar to pitch or to be under normal stress, we verify that there is a coupling between the longitudinal and the vertical motions, and that a positive normal stress (tension) has a positive effect on the stability, while a negative normal stress (compression) has a negative effect on the stability.

I. Introduction

Vertical take off and landing rotorcrafts, with hovering capabilities, provide a platform for transportation of cargos in dangerous and cluttered environments [1]. In cluttered environments, transportation with a single UAV may be the only feasible option, while transportation with multiple UAVs is primarily necessary when the cargo exceeds the individual UAVs' payload capacity. However, transportation with multiple UAVs is inevitable if one wishes to control the pose of the cargo: in particular, controlling the pose of a bar requires a minimum of two UAVs, while controlling the pose of a generic rigid body requires a minimum of three UAVs [2].

Using tethers in conjunction with UAVs can serve different and distinct purposes. Tethers/cables may be used to supply power or fuel to the UAV and thus to extend its flight time, or they may be used to provide an uninterrupted data transmission link [3]–[5]. However, in this paper, the purpose of the cables is to physically couple one or more UAVs to a cargo: when the cables are slack, the cargo is free of actuation; on the contrary, when they are taut, the cables provide an actuation medium for stabilizing the pose of the cargo. In this work, we assume that the cables are always taut, and thus that they behave as massless rigid links. A hybrid model, as in [6]–[8], can provide a more complete description of the dynamics of tethered transportation by accounting for the hybrid behaviour of the cables. However, the focus of this paper is on the control design and analysis of the local closed-loop behavior, which does not require a complete hybrid model of the system.

Manipulator-endowed transportation [9]–[11] provides an alternative to tethered transportation. However, tethered transportation is mechanically simple and inexpensive, while robotic manipulators are heavy and therefore diminish the useful payload capacity a UAV can carry. Several control strategies for slung-load transportation, i.e., tethered transportation of a point-mass cargo by a single UAV, are found in the literature: the load swing can be dampened by appropriately planning trajectories, or by using vision and force measurements [12]–[16]; compensating for unknown model parameters can also be accomplished [17], [18]; and, when the point-mass cargo exceeds the allowed UAV's payload, cooperative tethered transportation becomes imperative [19]–[21].

This paper, on the other hand, focuses on transportation of a non-point-mass cargo. Control laws with an extended domain of operation and an extended domain of attraction are found in the literature [22]–[24], which can deal with asymmetries of the system but which lack experimental validation. On the other hand, cooperative transportation of rigid body cargos using simpler control laws has been tested and validated under various symmetry conditions (where UAVs are identical, cables are of the same length, and contact points are symmetrically distributed on the cargo) [2], [25]–[28]. We emphasize that aerial cooperative tethered transportation comes with multiple degrees of freedom, which can be exploited to, for example, minimize the internal forces applied on the cargo [29], [30]. In this manuscript, we focus on stabilization of a rod-like object tethered to two UAVs, as pictured in Fig. 1.

This problem has also been considered in [26], [31]–[33]. In [33], a master-slave approach for the two UAVs is adopted, where the UAV slave estimates the cable force exerted on itself. In [26], vision is used to autonomously estimate the bar's pose. In [31], [32], relations on the UAVs' PID gains are provided for which stability – regarding the bar's pose stabilization – is guaranteed. We note that [26], [31]–[33] take the system to be symmetric and/or stabilize the bar on the horizontal plane

The authors are with the School of Electrical Engineering, KTH Royal Institute of Technology, SE-100 44, Stockholm, Sweden. {ppereira, dimos}@kth.se. This work was supported by the EU H2020 Research and Innovation Programme under GA No.644128 (AEROWORKS), the Swedish Research Council (VR), the Swedish Foundation for Strategic Research (SSF) and the KAW Foundation.

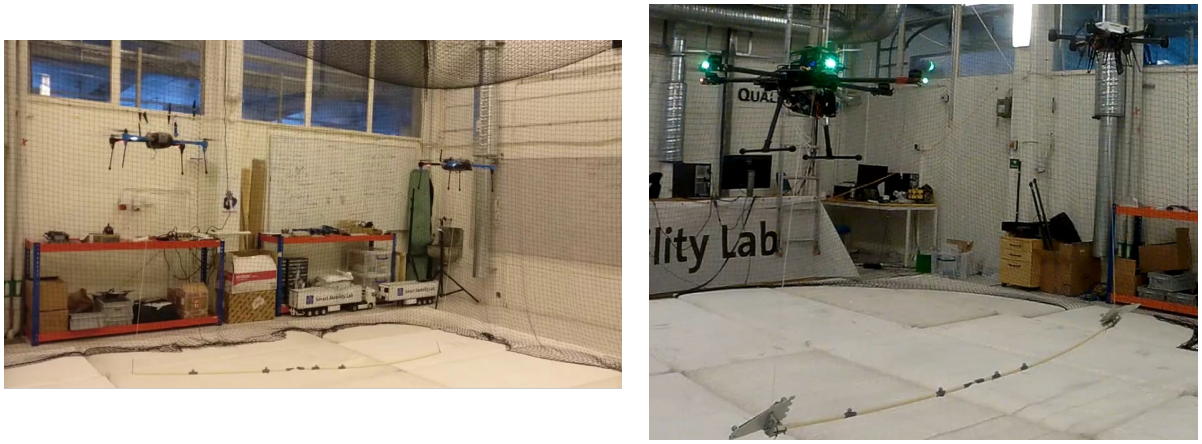

(a) Symmetric system, with two identical aerial vehicles and cables of the same length [31]

(b) Non-symmetric system, with two heterogeneous aerial vehicles, with cables of different lengths [32].

Fig. 1: Tethered transportation of a rod-like object by two aerial vehicles.

and under no normal stress; whereas, in this paper, we relax both of these conditions. We perform an analysis similar to that in [6], [34], [35], where we linearize the system, and derive conditions on the gains that guarantee exponential stability regarding the stabilization of the bar's pose. We note that the state-space of the system is a manifold, and for that reason we provide an analysis tool that allows us to linearize the vector field around a point in the state-space without having to provide a parameterization of the manifold.

The results of this paper are partially based on [31], [32], with the first focusing on the symmetric case, and the second focusing on the asymmetric case. This paper's main contributions, which we list next, are also the distinguishing factors with respect to [31], [32]. (i) We provide a detailed model derivation of the system, based on a Newtonian approach, and we show that the open-loop vector field is invariant to translations and rotations around the vertical direction; we also describe and parametrize the open-loop equilibrium points and equilibrium inputs, from which we derive the necessity of integral action terms in the vertical direction of each UAVs' control law – Section III. (ii) We construct a bounded PID-like control law, which guarantees that physical input limitations can be met, and that the desired UAVs' attitude are always well-defined; we then show that the closed-loop equilibria of interest are entirely parameterizable with just two parameters, namely the desired pitch angle of the bar ($\theta_\star$), and the desired normal stress to be exerted on the bar ($F_\star$) – Section IV. (iii) When $(\theta_\star, F_\star) = (0, 0)$, we show that the system's motion can be broken down into three decoupled motions (vertical, longitudinal and lateral), with each motion being composed of two sub-motions (one linear and one angular) – Sections VI-C and VI-D. When $\theta_\star \neq 0$ or $F_\star \neq 0$, we show that the longitudinal and the vertical motions are no longer decoupled; we also find out that a bar under tension, as opposed to a bar under compression, is beneficial when it comes to stability – Sections VI-E and VI-F. For all the different cases, we provide conditions on the control law PID gains that guarantee that each and every motion/sub-motion is asymptotically stable, and therefore that the equilibrium of the non-linear system is (locally) exponentially stable. We also provide conditions, based on the system's physical parameters, that describe *good* and *bad* types of asymmetries: e.g., it is better for the heavier vehicle to be attached to the shorter cable, in the sense that stability is guaranteed by a smaller proportional gain.

II. Notation

The map $\mathcal{S} : \mathbb{R}^3 \ni x \mapsto \mathcal{S}(x) \in \mathbb{R}^{3\times 3}$ yields a skew-symmetric matrix and it satisfies $\mathcal{S}(a)\, b = a \times b$, for any $a, b \in \mathbb{R}^3$. $\mathbb{S}^2 := \{x \in \mathbb{R}^3 : x^T x = 1\}$ denotes the set of unit vectors in $\mathbb{R}^3$. We denote $A_1 \oplus \cdots \oplus A_n$ as the block diagonal matrix with block diagonal entries A_1 to A_n (square matrices). We denote by $e_1, \cdots, e_n \in \mathbb{R}^n$ the canonical basis vectors in $\mathbb{R}^n$, for some $n \in \mathbb{N}$. Given some $n, m \in \mathbb{N}$, and a function $f : \mathbb{R}^n \ni a \mapsto f(a) \in \mathbb{R}^m$, $Df : \mathbb{R}^n \ni a \mapsto Df(a) \in \mathbb{R}^{m\times n}$ denotes the derivative of f.

III. Problem Description

Consider the system illustrated in Fig. 2, with two VTOL aerial vehicles, a one dimensional bar and two cables connecting the aerial vehicles to distinct contact points on the bar. Fig. 2 provides a two-dimensional picture of the real system, as shown in Fig. 1, but the modeling we describe next is three dimensional. Hereafter, and for brevity, we refer to this system as UAVs-bar system. We denote by $p_1, p_2, p \in \mathbb{R}^3$ and by $v_1, v_2, v \in \mathbb{R}^3$ the UAVs' and the bar's center-of-mass positions and velocities; by $n, \omega \in \mathbb{R}^3$ the bar's angular position (orientation) and angular velocity; and by $r_1, r_2 \in \mathbb{S}^2$ the UAVs' thrust body directions. As for physical constants, we denote by $m_1, m_2, m > 0$ the UAVs' and bar's masses; by $J > 0$ the bar's moment of inertia

(w.r.t. the bar's center-of-mass); by $l_1, l_2 > 0$ the cables' lengths; and, finally, by $d_1, d_2 \in \mathbb{R}$ the contact points on the bar at which the cables are attached to (d_i is positive if the contact point i is away from the bar's center-of-mass by a distance $|d_i|$ and along the bar's direction, i.e., along $+n \in \mathbb{S}^2$; and, it is negative if it is away from the bar's center-of-mass along the opposite direction, i.e, along $-n \in \mathbb{S}^2$ – see Fig. 2).

Finally, we denote by $u_1, u_2 \in \mathbb{R}^3$ the input forces on the UAVs-bar system: for $i \in \{1, 2\}$, $\bar{u}_i := U_i r_i := u_i^T r_i r_i$ is the UAV i input force, where the throttle U_i is taken as the inner product between the input u_i and the UAV's thrust direction r_i (one may think of u_i as the desired value for $\bar{u}_i$).

Consider then the position variables

$$z_p := \begin{bmatrix} p \\ n \\ p_1 \\ p_2 \end{bmatrix} = \begin{bmatrix} \text{linear position of bar} \in \mathbb{R}^3 \\ \text{angular position of bar} \in \mathbb{R}^3 \\ \text{linear position of UAV 1} \in \mathbb{R}^3 \\ \text{linear position of UAV 2} \in \mathbb{R}^3 \end{bmatrix}, \tag{1a}$$

and the corresponding velocity variables

$$z_v := \begin{bmatrix} v \\ \omega \\ v_1 \\ v_2 \end{bmatrix} = \begin{bmatrix} \text{linear velocity of bar} \in \mathbb{R}^3 \\ \text{angular velocity of bar} \in \mathbb{R}^3 \\ \text{linear velocity of UAV 1} \in \mathbb{R}^3 \\ \text{linear velocity of UAV 2} \in \mathbb{R}^3 \end{bmatrix}. \tag{1b}$$

For brevity, given the quantities described above, denote

$$z := (z_p, z_v) \in \mathbb{R}^{24} \tag{2}$$

$$u := (u_1, u_2) \in \mathbb{R}^6 \tag{3}$$

where z in (2) is used next as the state of the UAVs-bar system, and u in (3) is used next as the input to the UAVs-bar system. Given the position and the velocity variables in (1a) and (1b), the system kinematics Z_p are given by

$$\dot{z}_p = Z_p(z) :\Leftrightarrow \dot{z}_p = \underbrace{\left(I_3 \oplus \mathcal{S}\left(-n\right) \oplus I_3 \oplus I_3\right)}_{=:\bar{Z}_p(z_p) \in \mathbb{R}^{12 \times 12}} z_v \tag{4a}$$

$$\Leftrightarrow \begin{bmatrix} \dot{p} \\ \dot{n} \\ \dot{p}_1 \\ \dot{p}_2 \end{bmatrix} = \begin{bmatrix} v \\ \mathcal{S}\left(\omega\right) n \\ v_1 \\ v_2 \end{bmatrix}. \tag{4b}$$

Consider now the map $f : \mathbb{R}^{24} \ni z \mapsto f(z) \in \mathbb{R}^6$, which, when equal to 0_6, encapsulates the constraints illustrated in Fig. 2, defined as

$$f(z) := \begin{bmatrix} f_1(z_p) \\ f_2(z_p) \\ f_3(z_p, z_v) \\ f_4(z_p, z_v) \\ f_5(z_p) \\ f_6(z_p, z_v) \end{bmatrix} := \begin{bmatrix} \frac{\|p + d_1 n - p_1\|^2}{l_1^2} - 1 \\ \frac{\|p + d_2 n - p_2\|^2}{l_2^2} - 1 \\ \frac{(p + d_1 n - p_1)^T (v + d_1 \mathcal{S}(\omega) n - v_1)}{l_1^2} \\ \frac{(p + d_2 n - p_2)^T (v + d_2 \mathcal{S}(\omega) n - v_2)}{l_2^2} \\ n^T n - 1 \\ n^T \omega \end{bmatrix} = \begin{bmatrix} \cdots \\ \cdots \\ Df_1(z_p) \bar{Z}_p(z_p) z_v \\ Df_2(z_p) \bar{Z}_p(z_p) z_v \\ \cdots \\ \cdots \end{bmatrix}. \tag{5}$$

Specifically, (the constraints' nomenclature we adopt here is the standard one; see, f.e., [36])

- f_1 and f_2 are geometric constraints imposed by the cables, which require that the distance between each contact point on the bar and the corresponding UAV is equal to the corresponding cable length.
- f_3 and f_4 are kinematic (holonomic) constraints which follow from differentiation of the previous two geometric constraints: that is, $f_3(z_p, z_v) = Df_1(z_p)\dot{z}_p \overset{(4a)}{=} Df_1(z_p) Z_p(z)$ and $f_4(z_p, z_v) = Df_2(z_p)\dot{z}_p \overset{(4a)}{=} Df_2(z_p) Z_p(z)$.
- f_5 is a geometric constraint which implies that the bar's angular position n is given by a unit vector[1].
- And f_6 is a kinematic (nonholomonic) constraint which implies that the bar's angular velocity ω is orthogonal to the bar's angular position n, and thus that the bar does not rotate around itself.

The necessity for specifying the constraints is two-fold. First, it allows us to define the state-space and the tangent set to each point in the state-space; this, in turn, will allow us to determine the tensions in each cable. Secondly, when linearizing the closed-loop vector field around the desired equilibrium, the constraints as specified in the map f in (5) play a crucial role in examining whether the Jacobian matrix is Hurwitz or not (see Section VI).

[1]We do not need to include the kinematic (holonomic) constraint which follows from differentiation, since it is satisfied irrespectively of z: indeed, $Df_5(z_p)\dot{z}_p(z) \overset{(4a)}{=} Df_5(z_p) Z_p(z) = 2n^T \mathcal{S}\left(\omega\right) n = 0$ for all $n, \omega \in \mathbb{R}^3$.

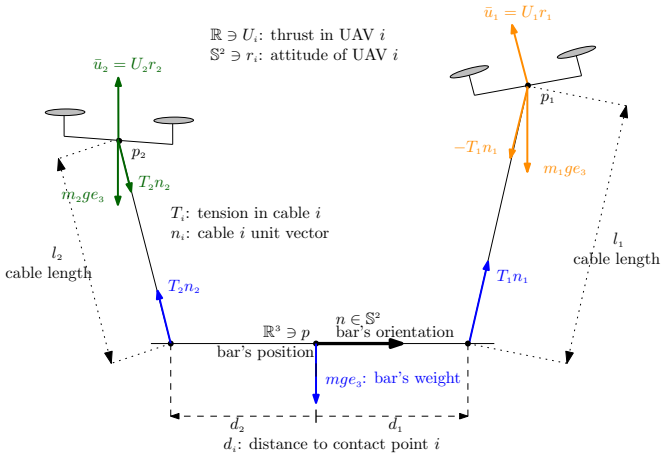

Fig. 2: Modeling of UAVs-bar system (given the bar's orientation, $d_1 > 0$ and $d_2 < 0$).

The constraints defined in (5) give rise to the state space

$$\mathbb{Z} := \{z \in \mathbb{R}^{24} : f(z) = 0_6\}, \tag{6}$$

which is a manifold of dimension $18 = 24 - 6$. The same constraints also give rise to the tangent space to $\mathbb{Z}$ in (6) at any $z \in \mathbb{Z}$, given by

$$T_z\mathbb{Z} := \{\dot{z} \in \mathbb{R}^{24} : Df(z)\dot{z} = 0_6\}, \tag{7}$$

where we recall that $Df(z) \in \mathbb{R}^{6\times 24}$ is the derivative of f at z.

Given an appropriate input $u : \mathbb{R}_{\geq 0} \to \mathbb{R}^6$, a system's trajectory $z : \mathbb{R}_{\geq 0} \ni t \mapsto z(t) \in \mathbb{Z}$ evolves according to

$$\dot{z}(t) = Z(z(t), u(t)), z(0) \in \mathbb{Z}, \tag{8a}$$

where the vector field $Z : \mathbb{Z} \times \mathbb{R}^6 \ni (z, u) \mapsto Z(z, u) \in \mathbb{R}^{24}$ is given by

$$\dot{z} = Z(z, u) :\Leftrightarrow \begin{bmatrix} \dot{z}_p \\ \dot{z}_v \end{bmatrix} = \begin{bmatrix} Z_p(z) \\ Z_v(z, u) \end{bmatrix}, \tag{8b}$$

with the kinematics Z_p defined in (4), and with the dynamics Z_v corresponding to the linear and the angular accelerations. The net force applied on a point-mass determines the rate of change of its linear momentum, while the net torque applied on a rigid-body determines the rate of change of its angular momentum; in turn, the change in linear/angular momentum determines the change in linear/angular acceleration. The forces and their application points are depicted in Fig. 2, which allows us to write down the dynamics Z_v of the system. For that purpose, and for convenience, consider the shorthands

$$n_i \equiv \frac{p_i - (p + d_i n)}{l_i} \in \mathbb{S}^2, \tag{9a}$$

$$\mathcal{T}_i \equiv T_i(z, u) n_i \in \mathbb{R}^3, \tag{9b}$$

where n_i is the unit vector associated to the cable i (indeed, $\frac{p_i-(p+d_i n)}{l_i} \in \mathbb{S}^2$ for all $z \in \mathbb{Z}$ – see (5)); and where $T_i(z, u)$ is the tension on cable i (which depends on the state z and the input u).

Given the velocity variables, as introduced in (1b), the dynamics are then given by (below, g stands for the acceleration due to gravity)

$$\dot{z}_v = Z_v(z, u) :\Leftrightarrow \tag{10a}$$

$$\Leftrightarrow \begin{bmatrix} \dot{v} \\ \dot{\omega} \\ \dot{v}_1 \\ \dot{v}_2 \end{bmatrix} = \begin{bmatrix} \frac{\mathcal{T}_1}{m} + \frac{\mathcal{T}_2}{m} - ge_3 \\ \mathcal{S}(d_1 n)\frac{\mathcal{T}_1}{J} + \mathcal{S}(d_2 n)\frac{\mathcal{T}_2}{J} \\ \frac{u_1}{m_1} - \frac{\mathcal{T}_1}{m_1} - ge_3 \\ \frac{u_2}{m_2} - \frac{\mathcal{T}_2}{m_2} - ge_3 \end{bmatrix} |_{(9b)} \tag{10b}$$

$$\Leftrightarrow \begin{bmatrix} \dot{v} \\ \dot{\omega} \\ \dot{v}_1 \\ \dot{v}_2 \end{bmatrix} = \underbrace{\begin{bmatrix} -ge_3 \\ 0_3 \\ \frac{u_1}{m_1} - ge_3 \\ \frac{u_2}{m_2} - ge_3 \end{bmatrix}}_{=:\mathcal{G}(u)\in\mathbb{R}^{12}} + \underbrace{\begin{bmatrix} \frac{n_1}{m} & \frac{n_2}{m} \\ \mathcal{S}(d_1 n)\frac{n_1}{J} & \mathcal{S}(d_2 n)\frac{n_2}{J} \\ -\frac{n_1}{m_1} & 0_3 \\ 0_3 & -\frac{n_2}{m_2} \end{bmatrix}}_{=:\mathcal{N}(z_p)\in\mathbb{R}^{12\times 2}} |_{(9a)} \begin{bmatrix} T_1(z, u) \\ T_2(z, u) \end{bmatrix}, \tag{10c}$$

and where the explicit expression of the tensions $T_1(z,u), T_2(z,u)$ is described next (they are found in (13)). We emphasize that the tensions are internal forces – see Remark 1 – and therefore their expression must be found by exploring the constraints imposed on the system. Indeed, recall that the system is subject to the constraints in (5), which means that the state space $\mathbb{Z}$ in (6) must be invariant with respect to the vector field Z, and, therefore, that

$$Z(z,u) \in T_z\mathbb{Z} \text{ for all } (z,u) \in \mathbb{Z} \times \mathbb{R}^6, \tag{11}$$

which is important in determining the tensions in the cables. Recalling (7), it follows from (11) that six constraints are imposed on the vector field Z. The satisfaction of the constraints that follow from the (three) geometric constraints is immediate (since these correspond to the kinematic holonomic constraints already included in (5)). The satisfaction of the constraint that follows from the non-holonomic kinematic constraint follows from the fact that $\dot{\omega}$ in (10b) is orthogonal to n ($\frac{d}{dt} n^T\omega = \dot{n}^T\omega + n^T\dot{\omega} \overset{(4b)}{=} n^T\mathcal{S}(\omega)^T\omega + n^T\dot{\omega} \overset{(10b)}{=} 0$). Finally, it remains to verify the satisfaction of the constraints that follow from the holonomic kinematic constraints: to be specific, these constraints read as (note that $D_2 f_3(z_p, z_v) = Df_1(z_p)\bar{Z}_p(z_p)$ and $D_2 f_4(z_p, z_v) = Df_2(z_p)\bar{Z}_p(z_p)$– see (5)),

$$\begin{bmatrix} D_1 f_3(z_p,z_v)\dot{z}_p + D_2 f_3(z_p,z_v)\dot{z}_v \\ D_1 f_4(z_p,z_v)\dot{z}_p + D_2 f_4(z_p,z_v)\dot{z}_v \end{bmatrix} = \begin{bmatrix} 0 \\ 0 \end{bmatrix} \Leftrightarrow \tag{12a}$$

$$\overset{(4b),(10a)}{\Leftrightarrow} \begin{bmatrix} D_1 f_3(z_p,z_v)Z_p(z) + Df_1(z_p)\bar{Z}_p(z_p)Z_v(z,u) \\ D_1 f_4(z_p,z_v)Z_p(z) + Df_2(z_p)\bar{Z}_p(z_p)Z_v(z,u) \end{bmatrix} = \begin{bmatrix} 0 \\ 0 \end{bmatrix} \tag{12b}$$

$$\overset{(10c)}{\Leftrightarrow} \begin{bmatrix} D_1 f_3(z_p,z_v)Z_p(z) + Df_1(z_p)\bar{Z}_p(z_p)\mathcal{G}(u) \\ D_1 f_4(z_p,z_v)Z_p(z) + Df_2(z_p)\bar{Z}_p(z_p)\mathcal{G}(u) \end{bmatrix} + \begin{bmatrix} Df_1(z_p)\bar{Z}_p(z_p)\mathcal{N}(z_p) \\ Df_2(z_p)\bar{Z}_p(z_p)\mathcal{N}(z_p) \end{bmatrix} \begin{bmatrix} T_1(z,u) \\ T_2(z,u) \end{bmatrix} = \begin{bmatrix} 0 \\ 0 \end{bmatrix}, \tag{12c}$$

and therefore the tensions in the cables are given by

$$\begin{bmatrix} T_1(z,u) \\ T_2(z,u) \end{bmatrix} = (\mathcal{M}(z_p))^{-1}\mathcal{T}(z), \text{ where} \tag{13a}$$

$$\mathcal{M}(z_p) = \left(\begin{bmatrix} \frac{m}{m_1} & 0 \\ 0 & \frac{m}{m_2} \end{bmatrix} + \begin{bmatrix} 1 & n_1^T n_2 \\ n_1^T n_2 & 1 \end{bmatrix} + \frac{m d_1 d_2}{J} \begin{bmatrix} \frac{d_1}{d_2}\|a\|^2 & a^T b \\ a^T b & \frac{d_2}{d_1}\|b\|^2 \end{bmatrix} |^{a=\mathcal{S}(n)n_1}_{b=\mathcal{S}(n)n_2} \right) |_{(9a)} \in \mathbb{R}^{2\times 2}, \text{ and} \tag{13b}$$

$$\mathcal{T}(z) = \left(\begin{bmatrix} \frac{m}{m_1} n_1^T & 0_{1\times 3} \\ 0_{1\times 3} & \frac{m}{m_2} n_2^T \end{bmatrix} \begin{bmatrix} u_1 \\ u_2 \end{bmatrix} + m \begin{bmatrix} \frac{\|v_1 - (v + d_1\mathcal{S}(\omega)n)\|^2}{l_1} \\ \frac{\|v_2 - (v + d_2\mathcal{S}(\omega)n)\|^2}{l_2} \end{bmatrix} + m\|\omega\|^2 \begin{bmatrix} d_1 n^T n_1 \\ d_2 n^T n_2 \end{bmatrix} \right) |_{(9a)} \in \mathbb{R}^2, \tag{13c}$$

where the matrix $\mathcal{M}(z_p)$ is positive definite, and thus invertible, for all $(z_p, \cdot) \in \mathbb{Z}$.

Remark 1: The tensions $T_1(z,u) \in \mathbb{R}$ and $T_2(z,u) \in \mathbb{R}$, in (10c), are internal forces to the mechanical system, and, as such, they do not contribute to the change of linear and angular momentum of the system. Indeed, if we define the total linear and angular momenta[2], respectively,

$$P(z_v) := mv + \sum_{i\in\{1,2\}} m_i v_i \in \mathbb{R}^3, \tag{14a}$$

$$H(z_p, z_v) := J\omega + \sum_{i\in\{1,2\}} \mathcal{S}(p_i - p)\, m_i v_i \in \mathbb{R}^3, \tag{14b}$$

it is simple to verify that, for any $(z_p, z_v) \in \mathbb{Z}$, (recall (10c) which states that $\dot{z}_v$ is affine with respect to the tensions),

$$DP(z_v)\mathcal{N}(z_p) = 0_{3\times 2}, \tag{14c}$$

$$D_2 H(z_p, z_v)\mathcal{N}(z_p) = 0_{3\times 2}. \tag{14d}$$

That is, the rate of change of the total linear and angular momentum ($\frac{d}{dt}P(z_v) = DP(z_v)\dot{z}_v$ and $\frac{d}{dt}H(z_p,z_v) = D_1 H(z_p,z_v)\dot{z}_p + D_2 H(z_p,z_v)\dot{z}_v$) is independent of the tensions $T_1(z,u)$ and $T_2(z,u)$, which play a role in the dynamics as specified in (10c). We emphasize that this conclusion is independent of the explicit expression of $T_1(z,u)$ and $T_2(z,u)$, found in (13).

Remark 2: The vector field Z in (8b) is input affine, that is

$$\dot{z} = Z(z,u) \Leftrightarrow \begin{bmatrix} \dot{z}_p \\ \dot{z}_v \end{bmatrix} = \underbrace{\begin{bmatrix} Z_p(z) \\ A(z_p,z_v) \end{bmatrix}}_{\in\mathbb{R}^{24}} + \underbrace{\begin{bmatrix} 0_{12\times 6} \\ B(z_p) \end{bmatrix}}_{\in\mathbb{R}^{24\times 6}} u, \tag{15a}$$

[2]The angular momentum in (14b) is defined with respect to the bar's center-of-mass. However, the conclusion in (14d) holds if the angular momentum is expressed with respect to any other point.

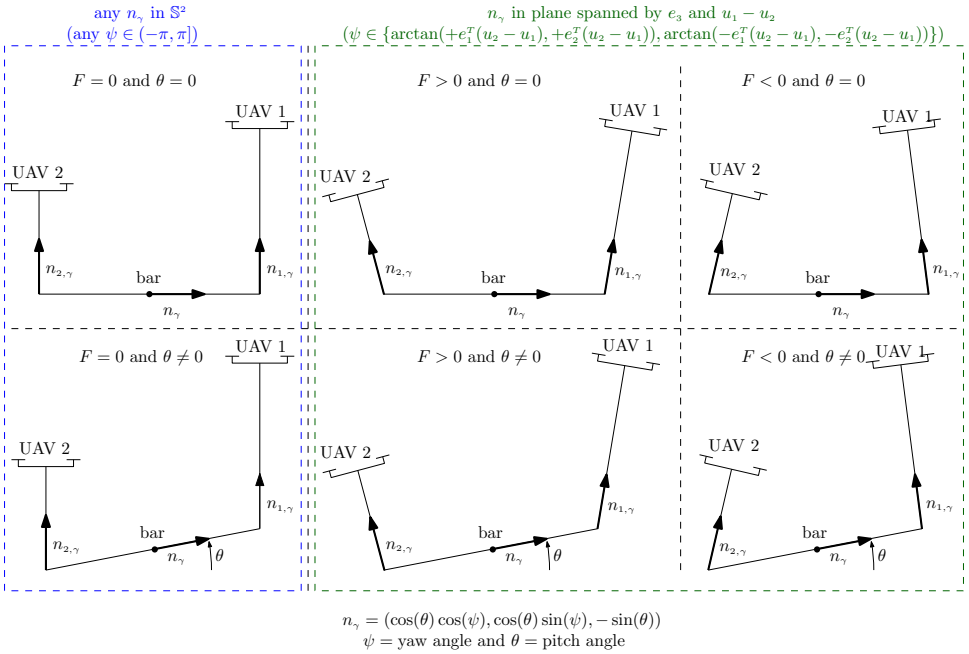

Fig. 3: Different equilibrium possibilities, for different values of the pitch angle of the bar – $\theta \in \left(-\frac{\pi}{2}, \frac{\pi}{2}\right)$ – and different values of be the normal force exerted on the bar – $F \in \mathbb{R}$. When $F > 0$, the bar is under tension; when $F < 0$, the bar is under compression; and, when $F = 0$, the bar is under no normal force.

where

$$A(z_p, z_v) := Z_v(z, 0_6) \in \mathbb{R}^{12}, \tag{15b}$$

$$B(z_p) := \begin{bmatrix} 0 & 0 \\ 0 & 0 \\ \frac{1}{m_1} & 0 \\ 0 & \frac{1}{m_2} \end{bmatrix} \otimes I_3 + \mathcal{N}(z_p)(\mathcal{M}(z_p))^{-1} \begin{bmatrix} \frac{m}{m_1} n_1^T & 0_{1\times 3} \\ 0_{1\times 3} & \frac{m}{m_2} n_2^T \end{bmatrix} |_{(9a)} \in \mathbb{R}^{12\times 6}, \tag{15c}$$

with $\mathcal{N}$ and $\mathcal{M}$ as defined in (10c) and (13b), respectively.

A. Equilibria

In the previous section, we specified the vector field that describes the motion of our system, i.e., $\dot{z} = Z(z, u)$. In this section, we specify the open-loop equilibria (non-exhaustive list however), i.e., given a constant input $u \in \mathbb{R}^6$, we determine the states $z \in \mathbb{Z}$ for which $0_{24} = Z(z, u)$. The open-loop equilibria we describe next are illustrated in Fig. 3.

As we verify next, in open-loop, there exists a continuum of equilibrium points, and therefore no such point is asymptotically stable. This is the main reason for closing the loop, under an appropriate control law, which we specify in Section IV. Under the proposed control law, the closed-loop equilibria is restricted to a smaller set when compared to the open-loop equilibria, which contains the desired equilibrium point as an isolated equilibrium point (and whose stability properties we study in Section VI).

In what follows, let $u \in \mathbb{R}^6$ be some chosen (constant) input, for which we wish to determine the possible open-loop equilibria. The equilibria set is given by $E_u := \{z \in \mathbb{Z} : Z(z, u) = 0_{24}\}$, with Z as vector field described in (8b). (Given that the vector field is input affine – see Remark 2, we can describe the equilibria set as $E_u := \{z \in \mathbb{Z} : z_v = 0_{12} \text{ and } 0_{12} = A(z_p, 0_{12}) + B(z_p)u\} = \{z \in \mathbb{Z} : z_v = 0_{12} \text{ and } A(z_p, 0_{12}) \in \text{Im}(B(z_p))\}$ – this, however, is not a helpful description). It follows from the first six equations in (10b) that (recall that the cables are connected to distinct contact points, i.e., $d_1 \neq d_2$)

$$\begin{bmatrix} 0_3 \\ 0_3 \end{bmatrix} = \begin{bmatrix} \frac{\mathcal{T}_1}{m} + \frac{\mathcal{T}_2}{m} - ge_3 \\ \mathcal{S}(d_1 n)\frac{\mathcal{T}_1}{J} + \mathcal{S}(d_2 n)\frac{\mathcal{T}_2}{J} \end{bmatrix} \Leftrightarrow \begin{bmatrix} mge_3 \\ (d_1 - d_2)Fn \end{bmatrix} = \begin{bmatrix} \mathcal{T}_1 + \mathcal{T}_2 \\ d_1\mathcal{T}_1 + d_2\mathcal{T}_2 \end{bmatrix} \text{ for any } F \in \mathbb{R} \tag{16a}$$

$$\Leftrightarrow \begin{bmatrix} \mathcal{T}_1 \\ \mathcal{T}_2 \end{bmatrix} = \begin{bmatrix} \frac{d_2}{d_2 - d_1} mge_3 + Fn \\ \frac{d_1}{d_1 - d_2} mge_3 - Fn \end{bmatrix} \text{ for any } F \in \mathbb{R}, \tag{16b}$$

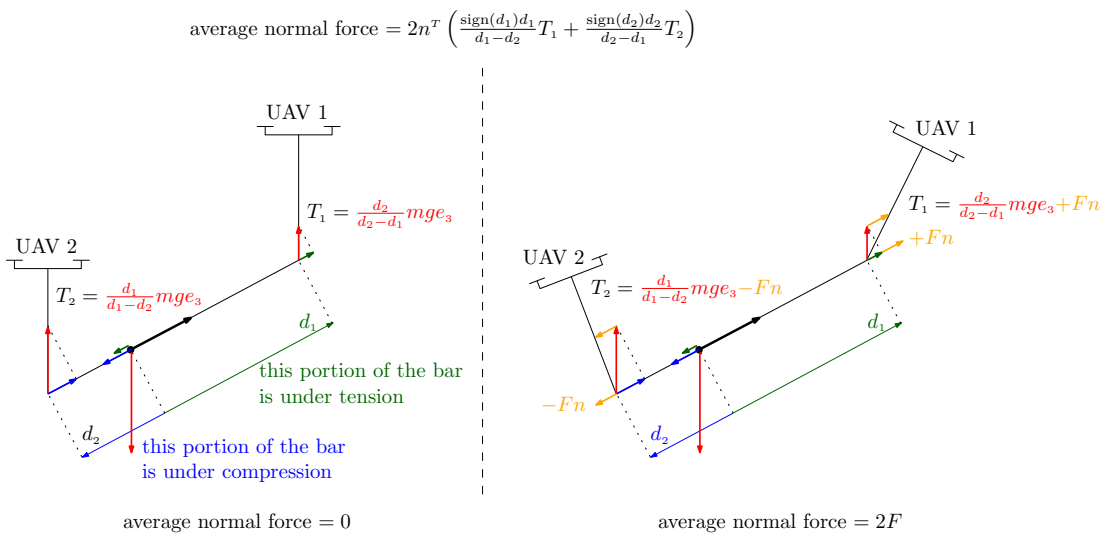

Fig. 4: Illustration of a bar under a zero and a non-zero average normal force.

where the meaning of F will become clear next. It follows from the final six equations in (10b) that

$$\begin{bmatrix}0_3\\0_3\end{bmatrix} = \begin{bmatrix}\frac{u_1}{m_1} - \frac{\mathcal{T}_1}{m_1} - ge_3\\ \frac{u_2}{m_2} - \frac{\mathcal{T}_2}{m_2} - ge_3\end{bmatrix} \Leftrightarrow \begin{bmatrix}\mathcal{T}_1\\\mathcal{T}_2\end{bmatrix} = \begin{bmatrix}u_1 - m_1ge_3\\ u_2 - m_2ge_3\end{bmatrix} \tag{16c}$$

$$\overset{(16b)}{\Leftrightarrow} \begin{bmatrix}u_1\\u_2\end{bmatrix} = \begin{bmatrix}m_1ge_3 + \frac{d_2}{d_2-d_1}mge_3 + Fn\\ m_2ge_3 + \frac{d_1}{d_1-d_2}mge_3 - Fn\end{bmatrix} \tag{16d}$$

$$\Leftrightarrow \begin{bmatrix}u_1 + u_2 - (m_1+m_2+m)ge_3\\ \frac{d_1}{d_1-d_2}(u_1 - m_1ge_3) + \frac{d_2}{d_1-d_2}(u_2 - m_2ge_3)\end{bmatrix} = \begin{bmatrix}0_3\\Fn\end{bmatrix}. \tag{16e}$$

That is, (16d) implies that for an input $(u_1, u_2) \in \mathbb{R}^3 \times \mathbb{R}^3$ to sustain an equilibrium:

- Each UAV needs to cancel its own weight (term m_ige_3 in (16d)).
- Each UAV needs to cancel some part of the bar's weight (term $\frac{d_i}{d_j-d_i}mge_3$ in (16d)), and where the fraction of weight depends on the contact points on the bar. In particular, if $d_1 = -d_2$, then each UAV carries half of the bar's weight; on the other hand, if $|d_i| \gg |d_j|$ then UAV j carries most of the bar's weight.
- One UAV applies some force $F \in \mathbb{R}$ along the bar's angular position n, while the other applies an opposite force. For simplicity, let $d_1 > 0$ and $d_2 < 0$: then, if the force $F > 0$, then the bar is under tension; if the force $F < 0$, then the bar is under compression; and finally, if $F = 0$, the bar is under no normal force/stress[3]. An illustration of a bar under a zero and a non-zero normal force is shown in Fig. 4.

Remark 3: Let $F = 0$ in (16b). If d_1, d_2 have opposite signs, then both cables are under tension. If d_1, d_2 have the same sign, then the cable with the smallest $|d_i|$ is under tension, and the one with the largest $|d_i|$ is under compression, which is not possible for a cable. For that reason, hereafter, we will assume that d_1 and d_2 have opposite signs. See Fig. 5 for a complete illustration of all the cases.

Proposition 4: Let $u \in \mathbb{R}^6 \Leftrightarrow (u_1, u_2) \in \mathbb{R}^3 \times \mathbb{R}^3$ be some chosen constant input, such that $e_3^T u_1 > m_1 g$ and $e_3^T u_2 > m_2 g$. Denote $E_u := \{z \in \mathbb{Z} : Z(z, u) = 0_{24}\}$ as the equilibria set for the input $u \in \mathbb{R}^6$, and (with (16e) in mind) denote also

$$\delta_1 \equiv u_1 + u_2 - (m_1 + m_2 + m)ge_3, \tag{17a}$$

$$\delta_2 \equiv \frac{d_1}{d_1 - d_2}(u_1 - m_1ge_3) + \frac{d_2}{d_1 - d_2}(u_2 - m_2ge_3). \tag{17b}$$

The following cases follow:

(i) If $\delta_1 \neq 0_3$, then $E_u = \emptyset$.

(ii) If $\delta_1 = 0_3$ and $\delta_2 = 0_3$, then

$$E_u = \Big\{(z_p, z_v) \in \mathbb{Z} : z_v = 0_{12} \text{ and, for any } p \in \mathbb{R}^3 \text{ and any } n \in \mathbb{S}^2,$$
$$z_p = (p, n, p + d_1n + l_1n_1, p + d_2n + l_2n_2)\Big\}\Big|_{n_i = \frac{u_i - m_ige_3}{\|u_i - m_ige_3\|} \in \mathbb{S}^2}, \tag{18a}$$

[3]Let $d_1 > 0$ and $d_2 < 0$ and assume we are at the equilibrium, where (16b) holds: then the average normal force on the bar is given by $2n^T\left(\frac{d_1}{d_1-d_2}T_1 - \frac{d_2}{d_2-d_1}T_2\right) = 2F$.

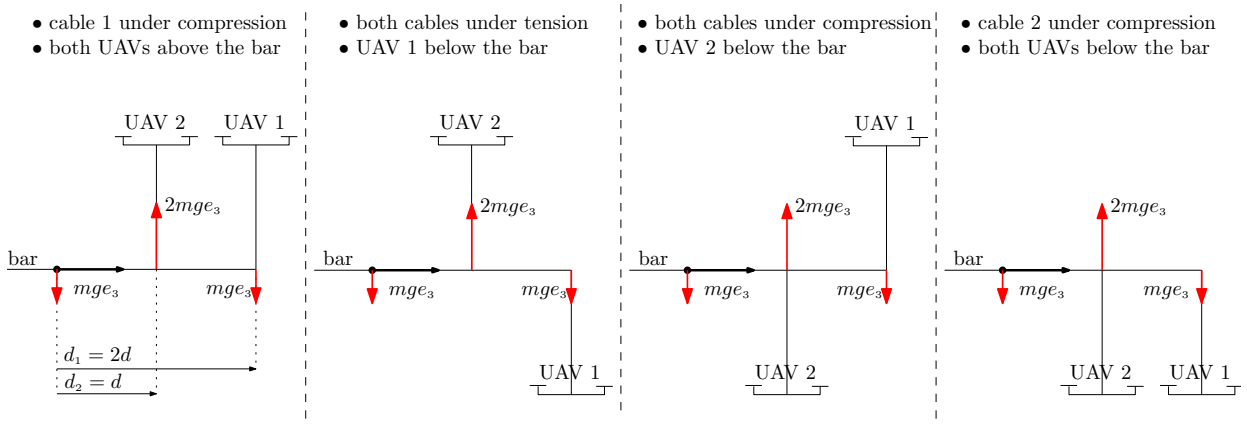

Fig. 5: If d_1 and d_2 have the same sign, then either one cable is under compression (not feasible), or one UAV needs to be "below" the bar. Configurations on the left are not considered in Proposition 4 (which requires that $e_3^T u_i > m_i g$, i.e., it requires that both UAVs are above the bar); and the configuration on the left is not feasible since cable 1 is not under tension.

where n_i is well-defined because $e_3^T u_i > m_i g \Rightarrow \|u_i - m_i g e_3\| \neq 0$.

(iii) If $\delta_1 = 0_3$ and $\delta_2 \neq 0_3$, then

$$E_u = \Big\{(z_p, z_v) \in \mathbb{Z} : z_v = 0_{12} \text{ and, for any } p \in \mathbb{R}^3 \text{ and for } n = \pm\frac{\delta_2}{\|\delta_2\|} \in \mathbb{S}^2,$$
$$z_p = (p, n, p + d_1 n + l_1 n_1, p + d_2 n + l_2 n_2)\Big\}\Big|_{n_i = \frac{u_i - m_i g e_3}{\|u_i - m_i g e_3\|} \in \mathbb{S}^2}, \tag{18b}$$

where n_i is well-defined for the same reason as in (ii), and where

$$n = \pm\frac{\delta_2}{\|\delta_2\|} = \pm\frac{u_1 - (m_1 + \frac{d_2}{d_2 - d_1} m) g e_3}{\|u_1 - (m_1 + \frac{d_2}{d_2 - d_1} m) g e_3\|} \qquad \because \delta_1 = 0_3, \tag{19a}$$
$$= \pm\frac{u_2 - (m_2 + \frac{d_1}{d_1 - d_2} m) g e_3}{\|u_2 - (m_2 + \frac{d_1}{d_1 - d_2} m) g e_3\|} \qquad \because \delta_1 = 0_3. \tag{19b}$$

Proof: We know that at an equilibrium, the input needs to satisfy (16e) for some $n \in \mathbb{S}^2$, i.e., $u_1 + u_2 = (m_1 + m_2 + m) g e_3 \Leftrightarrow \delta_1 = 0_3$. That is, at an equilibrium, the combined inputs need to compensate for the combined weight of the whole system. This proves item (i) in the Proposition.

The second condition in (16e) reads as $\delta_2 = Fn$. As such, when $\delta_2 = 0_3$, the bar at equilibrium is under no normal stress (i.e., $F = 0$), and the bar can take any attitude (i.e., n can be any unit vector). On the other hand, when $\delta_2 \neq 0_3$, there are two possibilities: either $F = +\|\delta_2\|$ and $n = +\frac{\delta_2}{\|\delta_2\|}$, or $F = -\|\delta_2\|$ and $n = -\frac{\delta_2}{\|\delta_2\|}$; that is, the bar's angular position is uniquely defined except for a sign, with the difference that, in the first case, the bar is under tension, and, in the second case, the bar is under compression (if $d_1 > 0$ and $d_2 < 0$; if, on the contrary, $d_1 < 0$ and $d_2 > 0$, then the conclusions are reversed).

In order to complete the proof of (ii) and (iii), we need to compute n_1 and n_2. In what follows, let $i \in \{1, 2\}$. Recall from (9b) that $n_i = \frac{\mathcal{T}_i}{\|\mathcal{T}_i\|}$ and $T_i = \|\mathcal{T}_i\|$[4]. It then follows immediately from (16c) that $n_i = \frac{u_i - m_i g e_3}{\|u_i - m_i g e_3\|}$, which is well defined owing to the fact that $e_3^T u_i > m_i g \Rightarrow \|u_i - m_i g e_3\| > 0$. It also follows that the tension on cable i is given by $T_i = \|u_i - m_i g e_3\| > 0$.

There is only one condition left unverified, namely (13a). However, recall that (13a) was obtained from (12c), and the satisfaction of (12c) is immediate since both $Z_p(z_p, z_v)$ and $Z_v(z, u)$ vanish for any $z \in E_u$. ■

Remark 5: Let $u : \mathbb{R} \to \mathbb{R}^6 \Leftrightarrow (u_1, u_2) : \mathbb{R} \to \mathbb{R}^3 \times \mathbb{R}^3$ be some chosen time-varying input, such that, for all $t \in \mathbb{R}$, $e_3^T u_1(t) > m_1 g$, $e_3^T u_2(t) > m_2 g$, $\delta_1(t) = 0_3$, and $\delta_2(t) \in \text{span}(n)$ for some $n \in \mathbb{S}^2$ (with δ_1 and δ_2 as defined in (17)). Then, conclusion (iii) of Proposition 4 follows. The only difference with respect to Proposition 4 is that the bar will be under a time-varying normal force, rather than a constant normal force.

Proposition 4 provides some insight into the problem. Firstly, there are two non-binding conditions (inequalities), namely $e_3^T u_1 > m_1 g$ and $e_3^T u_2 > m_2 g$ which guarantee that, at the equilibrium, both cables are pointing up ($e_3^T n_i = \frac{e_3^T u_i - m_i g}{\|u_i - m_i g e_3\|} > 0$). There are however three binding conditions (equalities), namely $\delta_1 = 0_3 \Leftrightarrow u_1 + u_2 = (m_1 + m_2 + m) g e_3$. It follows from the former that $e_3^T \delta_1 = 0 \Leftrightarrow e_3^T (u_1 + u_2) = (m_1 + m_2 + m) g$, which states that the combined inputs need to compensate for the combined weight of the whole system. This binding condition on the inputs is hard to satisfy since one does not know exactly the weights of the UAVs and of the bar; in experiments, it is therefore important to include, on each UAV, an integrator in the

[4]We can exclude the equilibrium possibility where $n_i = -\frac{\mathcal{T}_i}{\|\mathcal{T}_i\|}$ and $T_i = -\|\mathcal{T}_i\| < 0$, since the cables need to be under tensile forces.

vertical direction so that the latter binding condition can be satisfied. Two more binding conditions follow from $\delta_1 = 0_3$, namely $e_1^T\delta_1 = 0$ and $e_2^T\delta_1 = 0$: when $F = 0$ (no normal force applied on the bar), these conditions are met when $e_1^T u_i = e_2^T u_i = 0$ (no horizontal input from both UAVs), where the latter conditions are easy to satisfy (and the main reason for not including integrators in the horizontal components – see Section IV).

Proposition 4 also tells us that no equilibrium is asymptotically stable in open-loop, since E_u in (ii) and (iii) corresponds to a continuum of equilibrium points. However, when the condition $\delta_2 \neq 0_3$ is satisfied, the equilibrium angular position of the bar (i.e. n) is uniquely determined up to a sign: intuition suggests that one equilibrium attitude might be asymptotically stable – the one where the bar is under tension – while the diametrically opposed attitude might be unstable – the one where the bar is under compression. Based on the previous intuition, one might be tempted into trying to satisfy the condition $\delta_2 \neq 0_3$ where the bar is under the normal force $F \neq 0$. There is however one disadvantage if this option is pursued: note from (16d) that one UAV needs to provide $+Fn$ while the other needs to provide $-Fn$, which requires both synchrony and also accuracy. Since the controllers are distributed (i.e., one controller on each UAV), perfect synchrony is hard to accomplish. On the other hand, if the UAVs are heterogeneous, it is also hard to guarantee that one UAV provides $+Fn$, while the other provides $-Fn$. One possible solution to this problem is the inclusion of an integrator (on each of the UAVs' control law) along the bar's angular position.

In the experiments, only the scenario $\delta_2 = 0_3 \Leftrightarrow F = 0$ has been tested, that is, the scenario where the bar is under no normal force at equilibrium. For this scenario (see (16d)), it follows that $u_1 = m_1 g e_3 + \frac{d_2}{d_2 - d_1} m g e_3$ and that $u_2 = m_2 g e_3 + \frac{d_1}{d_1 - d_2} m g e_3$. That is, at equilibrium, the UAVs do not need to provide any horizontal input, but only a vertical input. This is the main reason for, later on, including an integrator along the vertical direction, but not along the horizontal directions.

Let us parametrize the equilibria in a more readable manner. With the above in mind, let

$$\gamma \in \Gamma :\Leftrightarrow (p_\gamma, n_\gamma, F_\gamma) \in \mathbb{R}^3 \times \mathbb{S}^2 \times \mathbb{R}, \tag{20}$$

where

- $p_\gamma \in \mathbb{R}^3$ is the desired linear position for the bar's center-of-mass;
- $n_\gamma \in \mathbb{S}^2$ is the desired angular position (orientation) for the bar;
- and $F_\gamma \in \mathbb{R}$ is the desired normal force to be exerted on the bar.

Briefly, γ is composed of the desired pose of the bar, and the desired normal force to be exerted on the bar. The variable γ in (20) is a six-dimensional variable[5] that allows us to parametrize the equilibrium input and the corresponding equilibria. That is, any point in the set

$$\{(z,u) \in \mathcal{Z} \times \mathbb{R}^6 : Z(z,u) = 0_{24}\} \Leftrightarrow \{(z,u) \in \mathcal{Z} \times \mathbb{R}^6 : u_1 + u_2 = (m_1 + m_2 + m) g e_3 \text{ and } z \in E_u\} \tag{21a}$$

can be parametrized by some $\gamma \in \Gamma$, i.e.,

$$\{(z,u) \in \mathcal{Z} \times \mathbb{R}^6 : Z(z,u) = 0_{24}\} \Leftrightarrow \{(z_\gamma, u_\gamma) \in \mathcal{Z} \times \mathbb{R}^6 : \gamma \in \Gamma\}, \tag{21b}$$

with (z_γ, u_γ) as described next (and which can be visualized in Fig. 3). The equilibrium input u_γ is parametrized by n_γ and F_γ as[6]

$$u_\gamma := \begin{bmatrix} u_{1,\gamma} \\ u_{2,\gamma} \end{bmatrix} := \begin{bmatrix} \left(m_1 + \frac{d_2}{d_2 - d_1} m\right) g e_3 + F_\gamma n_\gamma \\ \left(m_2 + \frac{d_1}{d_1 - d_2} m\right) g e_3 - F_\gamma n_\gamma \end{bmatrix} \tag{22}$$

while the equilibrium state z_γ is be parametrized as

$$z_\gamma := (z_{p,\gamma}, z_{v,\gamma}), \tag{23a}$$

$$z_{v,\gamma} := (v_\gamma, \omega_\gamma, v_{1,\gamma}, v_{2,\gamma}) := (0_3, 0_3, 0_3, 0_3), \tag{23b}$$

$$z_{p,\gamma} := (p_\gamma, n_\gamma, p_{1,\gamma}, p_{2,\gamma}) := \left(p_\gamma, n_\gamma, p_\gamma + d_1 n_\gamma + l_1 \frac{e_3 + \frac{d_2 - d_1}{d_2} \frac{F_\gamma}{mg} n_\gamma}{\left\| e_3 + \frac{d_2 - d_1}{d_2} \frac{F_\gamma}{mg} n_\gamma \right\|}, p_\gamma + d_2 n_\gamma + l_2 \frac{e_3 - \frac{d_1 - d_2}{d_1} \frac{F_\gamma}{mg} n_\gamma}{\left\| e_3 - \frac{d_1 - d_2}{d_1} \frac{F_\gamma}{mg} n_\gamma \right\|} \right). \tag{23c}$$

For the particular case when the bar is under no normal force, i.e., $F_\gamma = 0$, (22) and (23c) read more briefly as

$$\begin{bmatrix} u_{1,\gamma} \\ u_{2,\gamma} \end{bmatrix} := \begin{bmatrix} \left(m_1 + \frac{d_2}{d_2 - d_1} m\right) g e_3 \\ \left(m_2 + \frac{d_1}{d_1 - d_2} m\right) g e_3 \end{bmatrix}, \tag{24}$$

$$z_{p,\gamma} := (p_\gamma, n_\gamma, p_{1,\gamma}, p_{2,\gamma}) := (p_\gamma, n_\gamma, p_\gamma + d_1 n_\gamma + l_1 e_3, p_\gamma + d_2 n_\gamma + l_2 e_3). \tag{25}$$

[5]Instead of (20), one could define $(p, \psi, \theta, T) \in \mathbb{R}^3 \times (-\pi, \pi] \times \left[-\frac{\pi}{2}, \frac{\pi}{2}\right] \times \mathbb{R}$: the idea being that $n = (\cos(\theta)\cos(\psi), \cos(\theta)\sin(\psi), -\sin(\theta)) \in \mathbb{S}^2$ where ψ represents a yaw angle and θ represents a pitch angle – see Fig. 3.

[6]There are only three binding conditions on the input for equilibria to exist, namely that $\delta_1 = 0_3$. Since $u \in \mathbb{R}^6$, then we expect three degrees of freedom to exist: this agrees with the fact that u_γ in (22) only depends on $(n_\gamma, F_\gamma) \in \mathbb{S}^2 \times \mathbb{R}$, which provide the three degrees of freedom.

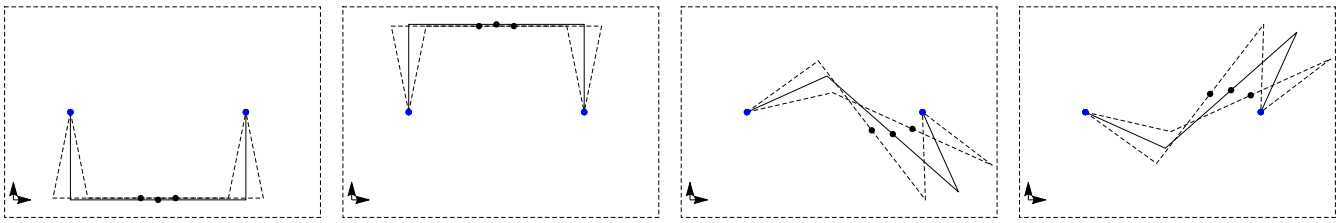

Fig. 6: Equilibrium configurations in full line, and perturbations to configuration in dashed (blue dots are the UAVs' linear positions, and the black dot is the bar's linear position). Potential energy of system (corresponding to the vertical component of the bar's linear position), from left to right: global minimum; global maximum; local minimum; local maximum. Only the leftmost configuration can be accomplished with cables, since the other configurations would require one or both cables to be under compressive forces.

Figure 3 illustrates the different possible equilibrium configurations.

Remark 6: Consider a pendulum-on-a-cart system – see illustration in Fig. 9, and let $n \in \mathbb{S}^2$ denote the unit vector pointing from the pendulum to the cart. This system has infinite open-loop equilibria, corresponding to configurations which maximize or minimize the potential energy: to be specific, either the pendulum is downwards ($e_3^T n = 1 > 0$) or upwards ($e_3^T n = -1 < 0$), while there are no restrictions in the linear position of the cart.

Like the pendulum-on-a-cart system, the UAVs-bar system also has infinite open-loop equilibria, with no restrictions on the linear position of the bar. Similarly, there are two equilibria: one where both n_1 and n_2 are pointing upward ($e_3^T n_1 > 0$ and $e_3^T n_2 > 0$), and which corresponds to the global minimum of the potential energy; and one where both n_1 and n_2 are pointing downward ($e_3^T n_1 < 0$ and $e_3^T n_2 < 0$), and which corresponds to the global maximum of the potential energy. However, unlike the pendulum-on-a-cart system, there may be more equilibria (for example, where $e_3^T n_1$ and $e_3^T n_2$ have opposite signs) corresponding to configurations where the potential energy is locally minimized or locally maximized. Figure 6 illustrates some of these possibilities.

In Proposition 4, we restrict $e_3^T u_1 > m_1 g \Leftrightarrow e_3^T n_1 > 0$ and $e_3^T u_2 > m_2 g \Leftrightarrow e_3^T n_2 > 0$ which precludes the other possible equilibria. Indeed, for all equilibria that do not globally minimize the potential energy of the system, either or both the tensions T_1 and T_2 are negative: that means these equilibria are not attainable with cables, which are only taut under tension; they are only attainable if the cables are replaced with rigid massless rods, which can undergo tensile and compressive forces. Finally, note that fixing the UAVs' positions does not guarantee that a sole stable equilibrium exists (as such, steering the UAVs to their desired position is not guaranteed to steer the whole system to its desired configuration).

B. Control objective: Pose stabilization of the bar

Before introducing the UAVs' attitude dynamics, let us describe the control objective pursued in this paper. The control goal is to design a control law that guarantees pose stabilization of the bar around a desired linear position p_γ and around a desired angular position n_γ, and such that the bar is under a desired normal force F_γ.

Problem 1: Let $\gamma \in \Gamma$, as in (20), be some chosen desired configuration. Consider then the vector field Z in (8b), the equilibrium state z_γ in (23), and the equilibrium input u_γ in (22). Design a control law $u_\gamma^{cl} : \mathbb{Z} \to \mathbb{R}^6$ satisfying $u_\gamma^{cl}(z_\gamma) = u_\gamma$ and such that z_γ is a (locally) exponentially stable equilibrium point of the closed loop vector field $\mathbb{Z} \ni z \mapsto Z(z, u_\gamma^{cl}(z)) \in T_z\mathbb{Z}$.

Remark 7: Consider the closed-loop vector field $z \mapsto Z(z, u_\gamma^{cl}(z))$ in Problem 1. It is clear that $z_\gamma \in \{z \in \mathbb{Z} : Z(z, u_\gamma^{cl}(z)) = 0_{24}\}$, i.e., the desired equilibrium point z_γ is indeed an equilibrium of the closed-loop system. We emphasize however that, given a control law u_γ^{cl}, there may exist other equilibria other than z_γ, i.e., there can exist $\tilde{\gamma} \neq \gamma$ such that $Z(z_{\tilde{\gamma}}, u_\gamma^{cl}(z_{\tilde{\gamma}})) = 0_{24}$. See Section IV and Fig. 7 for an example.

Remark 8: Recall (20). Without loss of generality, in Problem 1, we may assume that $p_\gamma = 0_3$ and that $e_2^T n_\gamma = 0$, i.e., we may assume that

$$\gamma = (p_\gamma, n_\gamma, F_\gamma) \text{ with } p_\gamma = 0_3 \text{ and } n_\gamma = (\cos(\theta), 0, -\sin(\theta)). \tag{26}$$

That is, we may assume that we wish to stabilize the bar's linear position around the origin, and to stabilize the bar's angular position orthogonally to the second inertial axis (corresponding to a vanishing yaw angle – see Fig. 3). Loosely speaking, this simplification can be made since the open-loop vector field is invariant to translations and rotations around the gravity (which is aligned with the third inertial axis). More precisely, given some translation $o \in \mathbb{R}^3$ and some rotation

$R \in \{R \in \mathbb{SO}(3) : Re_3 = e_3\}$, and given

$$z_a = (p_a, n_a, p_{1,a}, p_{2,a}, v_a, \omega_a, v_{1,a}, v_{2,a}) \in \mathbb{Z}, \tag{27a}$$
$$z_b = T_{(R,o)}(z_a) := (R(p_a - o), Rn_a, R(p_{1,a} - o), R(p_{2,a} - o), Rv_a, R\omega_a, Rv_{1,a}, Rv_{2,a}) \in \mathbb{Z}, \tag{27b}$$
$$u_a = (u_{1,a}, u_{2,a}) \in \mathbb{R}^6, \tag{27c}$$
$$u_b = (Ru_{1,a}, Ru_{2,a}) \in \mathbb{R}^6, \tag{27d}$$

it follows that (we emphasize that the map between z_a and z_b is invertible[7], and so is the map between u_a and u_b; that plays a key role in proving the equivalence below)

$$\dot{z}_a = Z(z_a, u_a) \Leftrightarrow \dot{z}_b = Z(z_b, u_b). \tag{28}$$

Proof of (28)*:* We prove (28) holds for the equations related to the linear velocity of UAV 1. Proving it holds for all other equations follows similar steps, which are, for that reason, omitted.

First, let us prove that the tensions, as defined in (13), are invariant with respect to translations and rotations, i.e., that $T_i(z_a, u_a) = T_i(z_b, u_b)$ for z_a, z_b, u_a, u_b as defined in (27) (in proving this equality, we do not need to invoke the property that $Re_3 = e_3$). First note, from (9a), that

$$\begin{aligned} n_{i,a} :=& \frac{p_{i,a} - (p_a + d_i n_a)}{l_i} \\ \overset{(\text{any } o \in \mathbb{R}^3)}{=}& \frac{(p_{i,a} - o) - ((p_a - o) + d_i n_a)}{l_i} \\ \overset{(\text{any } R \in \mathbb{SO}(3))}{=}& R^T \frac{R(p_{i,a} - o) - (R(p_a - o) + d_i R n_a)}{l_i} \\ =& R^T \frac{p_{i,b} - (p_b + d_i n_b)}{l_i} =: R^T n_{i,b}. \end{aligned}$$

From this fact, it follows immediately that $n_{1,a}^T n_{2,a} = n_{1,b}^T n_{2,b}$, that $\|\mathcal{S}(n_a) n_{i,a}\| = \|\mathcal{S}(R^T n_b) R^T n_{i,b}\| = \|\mathcal{S}(n_b) n_{i,b}\|$, and that $(\mathcal{S}(n_a) n_{2,a})^T (\mathcal{S}(n_a) n_{1,a}) = (\mathcal{S}(n_b) n_{2,b})^T (\mathcal{S}(n_b) n_{1,b})$; and, therefore, that $\mathcal{M}(z_{p,a}) = \mathcal{M}(z_{p,b})$ – see (13b). It is also the case that $n_{i,a}^T u_{i,a} = n_{i,b}^T u_{i,b}$, that $\|v_{i,a} - (v_a + d_i \mathcal{S}(\omega_a) n_a)\| = \|v_{i,b} - (v_b + d_i \mathcal{S}(\omega_b) n_b)\|$, that $\|\omega_a\| = \|\omega_b\|$, and that $n_a^T n_{i,a} = n_b^T n_{i,b}$. All together, it follows that $T_i(z_a, u_a) = T_i(z_b, u_b)$.

Recall now the linear acceleration equation of UAV 1 in (10c), and note that

$$\begin{aligned} \dot{v}_{1,a} =& \frac{u_{1,a}}{m_1} - \frac{T_1(z_a, u_a)}{m_1} n_{1,a} - g e_3 \Leftrightarrow \\ \Leftrightarrow R\dot{v}_{1,a} =& \frac{Ru_{1,a}}{m_1} - \frac{T_1(z_a, u_a)}{m_1} R n_{1,a} - g R e_3 \\ \overset{(Re_3 = e_3 \text{ and } n_{1,a} = R^T n_{1,b} \text{ and } T_1(z_a,u_a) = T_1(z_b,u_b))}{\Leftrightarrow} & \dot{v}_{1,b} = \frac{u_{1,b}}{m_1} - \frac{T_1(z_b, u_b)}{m_1} n_{1,b} - g e_3. \end{aligned}$$

Following similar steps for all other equations, one concludes that $\dot{z}_a = Z(z_a, u_a) \Leftrightarrow \dot{z}_b = Z(z_b, u_b)$, which completes the proof. ■

C. Attitude inner loop

In the previous subsection, the UAVs were assumed fully actuated, that is, we assumed each UAV could provide a three dimensional force. This assumption was taken so as to simplify the exposition of the modeling, and in this section, we explain how we model the fact that the UAVs are not fully actuated. In brief, each UAV has a thrust body direction (r_1 and r_2 in Fig. 2) along which thrust can be provided; and, we assume we have control over the thrust and the angular velocity of each UAV. For that purpose, recall the state, the constraints, and the state space previously defined in (2), (5) and (6), respectively. Define now the extended state, constraints, and state space

$$\bar{z} \in \mathbb{R}^{30} :\Leftrightarrow (z, r_1, r_2) \in \mathbb{R}^{24} \times \mathbb{R}^3 \times \mathbb{R}^3, \tag{29a}$$
$$\bar{f}(\bar{z}) := \begin{bmatrix} f(z) \\ f_7(r_1) \\ f_8(r_2) \end{bmatrix} := \begin{bmatrix} f(z) \\ r_1^T r_1 - 1 \\ r_2^T r_2 - 1 \end{bmatrix}, \tag{29b}$$
$$\bar{Z} := \{\bar{z} \in \mathbb{R}^{30} : \bar{f}(\bar{z}) = 0_8\} = \mathbb{Z} \times \mathbb{S}^2 \times \mathbb{S}^2. \tag{29c}$$

[7] $T_{(R,o)} \circ T_{(R^T, -Ro)} = \mathrm{id}_{\mathbb{Z}}$ and $T_{(R^T, -Ro)} \circ T_{(R,o)} = \mathrm{id}_{\mathbb{Z}}$.

For convenience, denote $\mathbb{R}^6_0 := \mathbb{R}^6 \backslash \{(0_3, \cdot), (\cdot, 0_3)\}$. Given an appropriate input $u : \mathbb{R}_{\geq 0} \to \mathbb{R}^6_0$, a system's trajectory $\bar{z} : \mathbb{R}_{\geq 0} \ni t \mapsto \bar{z}(t) \in \bar{\mathbb{Z}}$ evolves according to

$$\dot{\bar{z}}(t) = \bar{Z}(\bar{z}(t), u(t)), \bar{z}(0) \in \bar{\mathbb{Z}}, \tag{30a}$$

where the vector field $\bar{Z} : \bar{\mathbb{Z}} \times \mathbb{R}^6_0 \ni (\bar{z}, u) \mapsto \bar{Z}(\bar{z}, u) \in T_{\bar{z}}\bar{\mathbb{Z}}$ is given by

$$\dot{\bar{z}} = \bar{Z}(\bar{z}, u) :\Leftrightarrow \begin{bmatrix} \dot{z} \\ \dot{r}_1 \\ \dot{r}_2 \end{bmatrix} = \begin{bmatrix} Z\left(z, \begin{bmatrix} U_1 r_1 \\ U_2 r_2 \end{bmatrix}\right) \\ \mathcal{S}(\omega_1) r_1 \\ \mathcal{S}(\omega_2) r_2 \end{bmatrix} := \begin{bmatrix} Z\left(z, \begin{bmatrix} u_1^T r_1 r_1 \\ u_2^T r_2 r_2 \end{bmatrix}\right) \\ \mathcal{S}\left(k_{r,1}\mathcal{S}(r_1)\frac{u_1}{\|u_1\|}\right) r_1 \\ \mathcal{S}\left(k_{r,2}\mathcal{S}(r_2)\frac{u_2}{\|u_2\|}\right) r_2 \end{bmatrix}, \tag{30b}$$

where Z is the vector field defined in (8b). Let us give some insight into the vector field in (30b), and let $i \in \{1, 2\}$. UAV i provides a thrust U_i along its thrust body direction r_i: moreover, $U_i = u_i^T r_i$, and therefore $U_i r_i = u_i + \Pi(r_i) u_i$. That means UAV i provides the desired input u_i, apart from an error $\Pi(r_i) u_i$, which vanishes when the UAV's thrust direction r_i is aligned with the direction of the input u_i. On the other hand, UAV i has an angular velocity $\omega_i = k_{r,i}\mathcal{S}(r_i)\frac{u_i}{\|u_i\|}$, where $k_{r,i} > 0$ is the gain of its attitude inner loop. This angular velocity steers the UAV's thrust direction r_i towards the direction of the input u_i. To gain some intuition, let $u_i \in \mathbb{R}^3 \backslash \{0_3\}$ be some constant vector and define $r_i^\star = \frac{u_i}{\|u_i\|} \in \mathbb{S}^2$. Then, if $\dot{r}_i = \mathcal{S}(k_{r,i}\mathcal{S}(r_i) r_i^\star) r_i$, it follows that, for $V(r_i) = 1 - r_i^T r_i^\star \in [0, 2]$, $\dot{V}(r_i) = DV(r_i)\dot{r}_i = -k_{r,i} \|\mathcal{S}(r_i) r_i^\star\|^2 = -V(r_i)(2 - V(r_i)) \leq 0$, which implies that $\lim_{t\to\infty} r_i(t) = r_i^\star$ provided that $r_i(0) \neq -r_i^\star$. The attitude inner-loop gain $k_{r,i} > 0$ influences how fast the UAV's thrust body direction r_i is steered towards the direction of the input u_i.

Given an input satisfying $\delta_1 = 0_3 \Leftrightarrow u_1 + u_2 = (m_1 + m_2 + m) g e_3$, it is straightforward to verify that the open-loop equilibria for the vector field in (30b) is given by

$$\bar{E}_u = \left\{ \bar{z} \in \bar{\mathbb{Z}} : z \in E_u \text{ and } r_i = \pm \frac{u_i}{\|u_i\|} \right\}, \tag{31}$$

where the set E_u is that described in Proposition 4. The equilibria where $r_i = -\frac{u_i}{\|u_i\|}$ for any or both $i \in \{1, 2\}$ are unstable, and therefore not considered in the rest of this paper.

We can now formulate the problem treated in this paper, as an extension of Problem 1.

Problem 2: Let $\gamma \in \Gamma$ be some chosen desired configuration. Consider then the vector field $\bar{Z}$ in (30b), the equilibrium state z_γ in (23), and the equilibrium input u_γ in (22). Design a control law $u_\gamma^{cl} : \mathbb{Z} \to \mathbb{R}^6_0$ satisfying $u_\gamma^{cl}(z_\gamma) = u_\gamma$ and such that

$$\bar{z}_\gamma := (z_\gamma, r_{1,\gamma}, r_{2,\gamma}) := \left(z_\gamma, \frac{u_{1,\gamma}}{\|u_{1,\gamma}\|}, \frac{u_{2,\gamma}}{\|u_{2,\gamma}\|}\right) \tag{32}$$

is a (locally) exponentially stable equilibrium point of the closed loop vector field $\bar{\mathbb{Z}} \ni \bar{z} \mapsto \bar{Z}(\bar{z}, u_\gamma^{cl}(z)) \in T_{\bar{z}}\bar{\mathbb{Z}}$.

Remark 9: A similar remark to that in Remark 8 can be made at this point, that is, (below, T is as defined in (27))

$$\dot{\bar{z}}_a = \bar{Z}(\bar{z}_a, u_a) \Leftrightarrow \dot{\bar{z}}_b = \bar{Z}(\bar{z}_b, u_b), \text{ where} \tag{33}$$

$$\bar{z}_b = \bar{T}_{(R,o)}(\bar{z}_a) := (T_{(R,o)}(z_a), R r_{1,a}, R r_{2,a}) \in \bar{\mathbb{Z}} \tag{34}$$

which implies that the open-loop vector field $\bar{z} \mapsto \bar{Z}(\bar{z}, u)$ does not *see* the rotation and offset (R, o) (for any $o \in \mathbb{R}^3$ and any $R \in \{R \in \mathbb{SO}(3) : R e_3 = e_3\}$).

IV. Control Law

Let us break down the control law exposition in three subsections. In the first, we introduce a PD-like control law. In the second, we introduce and motivate the need for an integral action term along the vertical direction and for each UAV. In the third, we introduce a saturated version of the former control law, where the saturation guarantees that the control law is bounded and that the desired UAV attitude is well-defined. In the fourth and final subsection, we briefly explain how to force the UAVs to rotate the bar when its desired angular position is (close to) diametrically opposed to its desired angular position.

A. PD control law

Recall the problem statement in Problem 2, where a desired pose and normal force are chosen, encapsulated in $\gamma = (p_\gamma, n_\gamma, F_\gamma)$. For convenience, denote (hereafter, we assume that $n_\gamma \neq \pm e_3$, that is, that we do not require the bar to stand vertically)

$$R_{n_\gamma} \equiv \begin{bmatrix} \frac{\Pi(e_3) n_\gamma}{\sqrt{1 - (e_3^T n_\gamma)^2}} & \frac{\mathcal{S}(e_3) n_\gamma}{\sqrt{1 - (e_3^T n_\gamma)^2}} & e_3 \end{bmatrix} \in \mathbb{SO}(3), \text{ and} \tag{35a}$$

$$\gamma_\star \equiv (p_\star, n_\star, F_{\gamma_\star}), \text{ with } p_\star = 0_3 \in \mathbb{R}^3 \text{ and } n_\star = (|\cos(\theta_\star)|, 0, -\sin(\theta_\star)) \in \mathbb{S}^2, \tag{35b}$$

where $\theta_\star, F_\star \in \mathbb{R}$. We emphasize that the following holds:

$$R_{n_\gamma}^T e_3 = e_3, \tag{35c}$$

$$R_{n_\gamma}^T n_\gamma = \left(\sqrt{1-(e_3^T n_\gamma)^2}, 0, e_3^T n_\gamma\right) = n_\star \text{ for } \theta_\star = -\arcsin(e_3^T n_\gamma), \tag{35d}$$

$$R_{n_\gamma}^T u_{j,\gamma} \overset{(22)}{=} \left(m_j + \frac{d_j}{d_j - d_i} m\right) g R_{n_\gamma}^T e_3 \pm F_\gamma R_{n_\gamma}^T n_\gamma \overset{(35c),(35d)}{=} u_{j,\gamma_\star} \text{ for } j \in \{1,2\}. \tag{35e}$$

The necessity of R_{n_γ}, $\gamma_\star$ in (35a), (35b) will be clear next. In brief, the idea is that it will suffice to study $\gamma_\star$ in (35b) (characterized by two parameters, $\theta_\star$ and $F_\star$) instead of the γ in (20) (characterized by six parameters).

Given a γ (with $n_\gamma \neq \pm e_3$), consider then the PD-like control law with a feed-forward term given by

$$u_\gamma^{pd} : \mathbb{Z} \to \mathbb{R}^6, u_\gamma^{pd}(z) := \begin{bmatrix} u_{1,\gamma}^{pd}(z) \\ u_{2,\gamma}^{pd}(z) \end{bmatrix} := \underbrace{\begin{bmatrix} u_{1,\gamma} \\ u_{2,\gamma} \end{bmatrix}}_{\text{feedforward term in (22)}} + \underbrace{\begin{bmatrix} \tilde{u}_{1,\gamma}^{pd}(z) \\ \tilde{u}_{2,\gamma}^{pd}(z) \end{bmatrix}}_{\text{PD term}}, \tag{36}$$

where, for each UAV $j \in \{1,2\}$,

$$\begin{aligned} &\tilde{u}_{j,\gamma}^{pd}(z) := -m_j R_{n_\gamma}\left(K_p^j R_{n_\gamma}^T (p_j - p_{j,\gamma}) + K_d^j R_{n_\gamma}^T v_j\right) - m_j d_j e_3^T \left(k_{p,\psi}^j \mathcal{S}(n_\gamma)\, n + k_{d,\psi}^j \omega\right) R_{n_\gamma} e_2 \text{ where} \\ &K_p^j = k_{p,x}^j \oplus k_{p,y}^j \oplus k_{p,z}^j = \begin{bmatrix} k_{p,x}^j & 0 & 0 \\ 0 & k_{p,y}^j & 0 \\ 0 & 0 & k_{p,z}^j \end{bmatrix} \in \mathbb{R}^{3\times 3} \text{ and } K_d^j = k_{d,x}^j \oplus k_{d,y}^j \oplus k_{d,z}^j = \begin{bmatrix} k_{d,x}^j & 0 & 0 \\ 0 & k_{d,y}^j & 0 \\ 0 & 0 & k_{d,z}^j \end{bmatrix} \in \mathbb{R}^{3\times 3}, \end{aligned} \tag{37}$$

and where

- $p_{1,\gamma}, p_{2,\gamma} \in \mathbb{R}^3$ are the UAVs' desired equilibrium positions given in (23c);
- $k_{p,l}^j \in \mathbb{R}_{>0}$, for $l \in \{x, y, \mathrm{z}\}$, are positive gains related to the position feedback, respectively, of vehicle $j \in \{1,2\}$;
- $k_{d,l}^j \in \mathbb{R}_{>0}$, for $l \in \{x, y, \mathrm{z}\}$, are positive gains related to the velocity feedback, respectively, of vehicle $j \in \{1,2\}$;
- $k_{p,\psi}^j \in \mathbb{R}_{>0}$ and $k_{d,\psi}^j \in \mathbb{R}_{>0}$ are positive gains related to the angular position and angular velocity feedback.

Note that $\tilde{u}_\gamma^{pd}(z_\gamma) = 0_6$, and therefore $u_\gamma^{pd}(z_\gamma) = u_\gamma$, as required in Problem 2.

Let us provide some insight into the control law (36), and recall that we wish to steer the linear position of the bar p to p_γ and to steer the angular position of the bar n to n_γ. Finally, and for brevity, let us introduce the following nomenclature (where we make use of R_{n_γ} defined in (35a)):

- $R_{n_\gamma} e_1$ corresponds to the longitudinal direction, or x-direction – i.e., when seen from above, this direction is aligned with the desired angular position of the bar n_γ;
- $R_{n_\gamma} e_2$ corresponds to the lateral direction, or y-direction – i.e., when seen from above, this direction is orthogonal to the desired angular position of the bar n_γ;
- $R_{n_\gamma} e_3 = e_3$ corresponds to the vertical direction, or z-direction – i.e., the direction that is diametrically opposed to the gravity vector.

When $n_\gamma = e_1$ (or when $n_\gamma = (\cos(\theta), 0, -\sin(\theta))$), then $R_{n_\gamma} = I_3$, which simply implies that when the desired angular position is aligned with the first inertial axis, then the longitudinal direction corresponds to the first inertial axis, and the lateral direction corresponds to the second inertial axis.

The control law in (37) may be decomposed in three identifiable parts:

- The component along the longitudinal direction ($R_{n_\gamma} e_1$) is composed of two terms, one proportional and one derivative, that act as a spring-damper that brings the UAV to its desired longitudinal position. This component is expected to influence the longitudinal linear motion of the bar, and the longitudinal motion between the UAVs (which one may think of as a longitudinal angular motion).
- The component along the lateral direction ($R_{n_\gamma} e_2$) is composed of four terms: two terms (proportional and derivative) that act as a spring-damper that brings the UAV to its desired lateral position; and two other terms (proportional and derivative) that assist on bringing the bar to its desired angular position. This component is expected to influence the lateral linear and angular motion of the bar[8].
- Finally, the component along the vertical direction ($R_{n_\gamma} e_3$) is composed of two terms, one proportional and one derivative, that act as a spring-damper that brings the UAV to its desired vertical position. This component is expected to influence the vertical linear and angular motions of the bar[9].

Remark 10: Recall Remark 8, where we established that the open-loop vector field does not *see* translations and rotations around the gravity. Recall also (35). It is easy to verify that, for $j \in \{1,2\}$, (T as defined in (27))

$$u_{j,\gamma}^{pd}(z) = R_{n_\gamma} u_{j,\gamma_\star}^{pd}\left(T_{\left(R_{n_\gamma}^T, p_\gamma\right)}(z)\right), \tag{38}$$

[8]The lateral angular motions of the bar may be understood as a yaw motion.

[9]The vertical angular motion of the bar may be understood as a pitch motion.

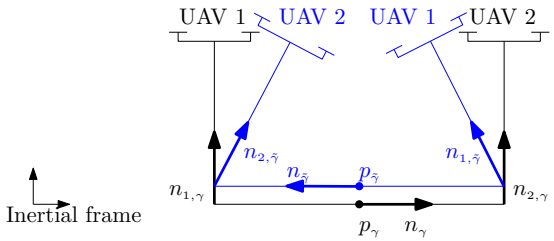

Fig. 7: The control law in (36) induces undesired closed-loop equilibria: in the figure, γ encodes the desired equilibrium point, while $\tilde{\gamma}$ encodes another (undesired) equilibrium point; that is, $\gamma, \tilde{\gamma} \in \{z \in \mathbb{Z} : Z(z, u^{pd}_\gamma(z)) = 0_{24}\}$ (a specific example is found in the Mathematica notebook file). Moreover, if the system starts close to the blue configuration, the control law in (36) *encourages* the UAVs to swap positions, and thus to make the bar rotate in the plane spanned by the UAVs; as opposed to *encouraging* the bar to rotate around the vertical direction.

for any $z \in \mathbb{Z}$ and any $\gamma \in \Gamma$; which combined with Remark 8 implies that the closed-loop vector field $z \mapsto Z(z, u^{pd}_\gamma(z))$ does not *see* the rotation and offset $(R^T_{n_\gamma}, p_\gamma)$. That means we can study only the closed-loop vector field $z \mapsto Z(z, u^{pd}_{\gamma_\star}(z))$, where we want to stabilize the bar around the origin, and aligned with the positive first-axis – see (35b). As such, when studying the different equilibrium possibilities encapsulated in γ, there are only two parameters that are worth studying, namely the desired normal force to be exerted on the bar $F_\star$ and the desired pitch angle of the bar $\theta_\star$.

The control law in (36) has three flaws that we address next:

- The terms $u_{1,\gamma}, u_{2,\gamma}$ are model dependent, and therefore sensitive to modeling identification errors (such as an unknown bar mass) – addressed in Subsection IV-B.
- The control law is unbounded: that is, $\|u^{pd}_{j,\gamma}(z)\|$ is arbitrarily large when the UAV's linear position p_j is arbitrarily far way from its desired linear position $p_{j,\gamma}$ – addressed in Subsection IV-C.
- When the bar's angular position n is (close to) diametrically opposed to its desired angular position n_γ, the control law *encourages* the UAVs to swap positions rather than *encouraging* the bar to rotate around the vertical direction. Moreover, it also induces undesired closed-loop equilibria (Fig. 7 illustrates this issue) – addressed in Subsection IV-D.

B. Integral action and PID control law

The control law in (36) is heavily dependent on the exact knowledge of model parameters. Suppose, for simplicity, that we wish the bar to be under no normal force, that is, $F_\gamma = 0$. Then, it follows from (24) that $u_{1,\gamma} = \left(m_1 g + \frac{d_2}{d_2 - d_1} m g\right) e_3$, that is, UAV 1 needs to have an exact knowledge of its weight, of the bar's weight, and of the contact points on the bar (an interchangeable conclusion may be drawn for UAV 2). Note, however, that only the third (vertical) component of $u_{1,\gamma}$ is model dependent, while the first and second (horizontal) components are zero and, therefore, model independent. This is the motivation for including an integral action in the vertical component of the control laws of each UAV (and to suppress such integral action in the horizontal components).

For that purpose, and with (29) in mind, define now the extended state, constraints, and state space

$$\tilde{z} \in \mathbb{R}^{32} :\Leftrightarrow (\bar{z}, \xi_{1,z}, \xi_{2,z}) \in \mathbb{R}^{30} \times \mathbb{R} \times \mathbb{R}, \tag{39a}$$

$$\tilde{f}(\tilde{z}) := \bar{f}(\bar{z}), \tag{39b}$$

$$\tilde{\mathbb{Z}} := \{\tilde{z} \in \mathbb{R}^{32} : \tilde{f}(\tilde{z}) = 0_8\} = \bar{\mathbb{Z}} \times \mathbb{R} \times \mathbb{R}, \tag{39c}$$

where $\xi_{1,z}, \xi_{2,z}$ are the integral action terms for UAVs $1, 2$.

Given an appropriate input $u : \mathbb{R}_{\geq 0} \to \mathbb{R}^6_0$, a system's trajectory $\tilde{z} : \mathbb{R}_{\geq 0} \ni t \mapsto \tilde{z}(t) \in \tilde{\mathbb{Z}}$ evolves according to

$$\dot{\tilde{z}}(t) = \tilde{Z}_\gamma(\tilde{z}(t), u(t)), \tilde{z}(0) \in \tilde{\mathbb{Z}}, \tag{40a}$$

where the vector field $\tilde{Z}_\gamma : \tilde{\mathbb{Z}} \times \mathbb{R}^6_0 \ni (\tilde{z}, u) \mapsto \tilde{Z}_\gamma(\tilde{z}, u) \in T_{\tilde{z}}\tilde{\mathbb{Z}}$ is given by

$$\dot{\tilde{z}} = \tilde{Z}_\gamma(\tilde{z}, u) :\Leftrightarrow \begin{bmatrix} \dot{\bar{z}} \\ \dot{\xi}_{1,z} \\ \dot{\xi}_{2,z} \end{bmatrix} = \begin{bmatrix} \bar{Z}(\bar{z}, u) \\ e_3^T(p_1 - p_{1,\gamma}) \\ e_3^T(p_2 - p_{2,\gamma}) \end{bmatrix}, \tag{40b}$$

where $\bar{Z}$ is the vector field defined in (30b). The integral action equations in (40b) enforce that an equilibrium can only be reached if the UAVs are at the desired height, i.e., if $e_3^T(p_i - p_{i,\gamma}) = 0$. Note also that the open-loop vector field in (40b) depends on γ, and thus the reason for indexing γ in $\tilde{Z}_\gamma$.

Remark 11: Recall Remark 9. It is easy to verify that (below, $\bar{T}$ is as defined in (34))

$$\dot{\tilde{z}}_a = \tilde{Z}_\gamma(\tilde{z}_a, u_a) \Leftrightarrow \dot{\tilde{z}}_b = \tilde{Z}_\gamma(\tilde{z}_b, u_b), \text{ where} \tag{41}$$

$$\tilde{z}_b = \tilde{T}_{(R,o)}(\tilde{z}_a) := \left(\bar{T}_{(R,o)}(\bar{z}_a), \xi_{1,z,a}, \xi_{2,z,a}\right) \tag{42}$$

which implies that the open-loop vector field $\tilde{z} \mapsto \tilde{Z}_\gamma(\tilde{z}, u)$ does not *see* the rotation and offset (R, o) (for any $o \in \mathbb{R}^3$ and any $R \in \{R \in \mathbb{SO}(3) : Re_3 = e_3\}$).

Remark 12: The integral action as defined in (40b) requires the knowledge of $e_3^T p_{i,\gamma}$ (and the measurement of $e_3^T p_i$), with $p_{i,\gamma}$ as defined in (23c). As such, if $e_3^T n_\gamma = 0$ and $F_\gamma = 0$ (top-left equilibrium configuration in Fig. 3), then the integral action requires only the knowledge of the cable lengths. On the other hand, if $e_3^T n_\gamma \neq 0$ or $F_\gamma \neq 0$ (the other equilibrium configurations in Fig. 3), then the integral action requires the knowledge of both the cable lengths as well as the distance of the contact points on the bar, i.e., d_1 and d_2.

Denote $\hat{u}_{1,\gamma}$ and $\hat{u}_{2,\gamma}$ as the best estimates of $u_{1,\gamma}$ and $u_{2,\gamma}$ known by UAVs 1 and 2, respectively[10]. With the control law (36) in mind, consider then the PID-like control law

$$\tilde{\mathbb{Z}} \ni \tilde{z} \mapsto u_\gamma^{pid}(\tilde{z}) := \begin{bmatrix} \hat{u}_{1,\gamma} \\ \hat{u}_{2,\gamma} \end{bmatrix} + \begin{bmatrix} \tilde{u}_{1,\gamma}^{pid}(\tilde{z}) \\ \tilde{u}_{2,\gamma}^{pid}(\tilde{z}) \end{bmatrix}, \text{ where} \tag{43a}$$

$$\begin{bmatrix} \tilde{u}_{1,\gamma}^{pid}(\tilde{z}) \\ \tilde{u}_{2,\gamma}^{pid}(\tilde{z}) \end{bmatrix} := \begin{bmatrix} \tilde{u}_{1,\gamma}^{pd}(z) \\ \tilde{u}_{2,\gamma}^{pd}(z) \end{bmatrix} + \begin{bmatrix} m_1 k_{i,z}^1 \xi_{1,z} e_3 \\ m_2 k_{i,z}^2 \xi_{2,z} e_3 \end{bmatrix}; \tag{43b}$$

where $\xi_{j,z}$ is the integral action term for UAV j; where $k_{i,z}^j$ the respective integral gain; and where $\tilde{u}_{j,\gamma}^{pd}$ is the PD control law in (37). It follows immediately that, for

$$\tilde{z}_\gamma := \begin{bmatrix} \bar{z}_\gamma \\ \xi_{1,z,\gamma} \\ \xi_{2,z,\gamma} \end{bmatrix} := \begin{bmatrix} \bar{z}_\gamma \\ \frac{1}{m_1 k_{i,z}^1} e_3^T (u_{1,\gamma} - \hat{u}_{1,\gamma}) \\ \frac{1}{m_2 k_{i,z}^2} e_3^T (u_{2,\gamma} - \hat{u}_{2,\gamma}) \end{bmatrix}, \tag{44}$$

it holds that $u_\gamma^{pid}(\tilde{z}_\gamma) = u_\gamma$, and therefore $\tilde{z}_\gamma$ is an equilibrium point of the closed loop vector field

$$\tilde{\mathbb{Z}} \ni \tilde{z} \mapsto \tilde{Z}_\gamma(\tilde{z}, u_\gamma^{pid}(\tilde{z})) \in T_{\tilde{z}}\tilde{\mathbb{Z}}. \tag{45}$$

Note that it is the purpose of the integral action terms to make sure the equality $u_\gamma^{pid}(\tilde{z}_\gamma) = u_\gamma$ is satisfied. Loosely speaking, the integral action terms $\xi_{1,z}, \xi_{2,z}$ evolve so as to compensate for the model mismatch; in particular, if all model parameters are exactly known by both UAVS, then $\xi_{1,z,\gamma} = \xi_{2,z,\gamma} = 0$ (even if all model parameters are exactly known, it is still a good practical solution to include integral action terms, as they provide robustness against other types of uncertainty). Finally, note that the control law u_γ^{pid} in (43) only differs from u_γ^{pd} in (36) along the vertical direction, and therefore the integral action terms are expected to influence only the vertical linear and vertical angular motions of the bar (and this is indeed the case when $\theta_\star = 0$ and $F_\star = 0$).

Remark 13: Recall Remark 11, where we established that the open-loop vector field does not *see* the rotation and offset (R, o). Recall also (35). It is easy to verify that, for $j \in \{1, 2\}$, (below, $\tilde{T}$ as defined in (42))[11]

$$u_{j,\gamma}^{pid}(\tilde{z}) = R_{n_\gamma} u_{j,\gamma_\star}^{pid}\left(\tilde{T}_{(R_{n_\gamma}^T, p_\gamma)}(\tilde{z})\right), \tag{46}$$

which combined with Remark 11 implies that the closed-loop vector field $\tilde{z} \mapsto \tilde{Z}_\gamma(\tilde{z}, u_\gamma^{pid}(\tilde{z}))$ does not *see* the rotation and offset $(R_{n_\gamma}^T, p_\gamma)$. That means we can study only the closed-loop vector field $\tilde{z} \mapsto \tilde{Z}_{\gamma_\star}(\tilde{z}, u_{\gamma_\star}^{pid}(z))$, where the want to stabilize the bar around the origin, and aligned with the positive first-axis – see (35b). As such, when studying the different equilibrium possibilities encapsulated in γ, there are only two parameters that are worth studying, namely the desired normal force to be exerted on the bar $F_\star$ and the desired pitch angle of the bar $\theta_\star$.

C. Bounded control law

From a practical perspective, it is important to guarantee that the control laws for each UAV are bounded, since each UAV has actuation limitations. On the other hand, from a well-posedness perspective, it is important to guarantee that the control laws for each UAV does not vanish. Indeed, recall from Section III-C, that the desired attitude for UAV i is given by $\frac{u_i}{\|u_i\|}$, which is only well defined provided that u_i does not vanish (which one is able to guarantee by appropriately saturating the proportional, derivative and integral terms).

[10]We emphasize that the term $\pm F_\gamma n_\gamma$ in (22) is model independent, but, as discussed in Section III-A, it requires synchrony between the UAVs. Moreover, the estimate $\hat{u}_{j,\gamma}$ only differs from the real $u_{j,\gamma}$ along the vertical direction, i.e., $\Pi(e_3)(\hat{u}_{j,\gamma} - u_{j,\gamma}) = 0_3$.

[11]Since $\Pi(e_3)(\hat{u}_{j,\gamma} - u_{j,\gamma}) = 0_3 \Leftrightarrow \hat{u}_{j,\gamma} = u_{j,\gamma} + ke_3$ for some $k \in \mathbb{R}$, it follows immediately from (35c)–(35e) that $R_{n_\gamma}^T \hat{u}_{j,\gamma} = \hat{u}_{j,\gamma_\star}$. This is necessary when proving (46).

Let σ be some positive constant and

$$\text{sat}_\sigma : \mathbb{R} \to [-\sigma, +\sigma] \tag{47}$$

be some saturation function, satisfying $\text{sat}_\sigma(0) = 0$, $0 < \text{sat}'_\sigma(\cdot) \leq 1$, $\text{sat}'_\sigma(0) = 1$ (for example, $x \mapsto \text{sat}_\sigma(x) = \frac{\sigma x}{\sqrt{\sigma^2+x^2}}$ is a possible saturation function).

With the control law u^{pid}_γ in (43) in mind, the real control law is then given by, for UAV $j \in \{1, 2\}$,

$$\begin{aligned} u^{pid}_{j,\gamma}(\tilde{z}) = \hat{u}_{j,\gamma} - m_j R_{n_\gamma} \begin{bmatrix} k^j_{p,x}\text{sat}_{\sigma^j_{p,x}}\left((R_{n_\gamma}e_1)^T(p_j - p_{j,\gamma})\right) + k^j_{d,x}\text{sat}_{\sigma^j_{d,x}}\left((R_{n_\gamma}e_1^T)v_j\right) \\ k^j_{p,y}\text{sat}_{\sigma^j_{p,y}}\left((R_{n_\gamma}e_2)^T(p_j - p_{j,\gamma})\right) + k^j_{d,y}\text{sat}_{\sigma^j_{d,y}}\left((R_{n_\gamma}e_2)^T v_j\right) \\ k^j_{p,z}\text{sat}_{\sigma^j_{p,z}}\left((R_{n_\gamma}e_3)^T(p_j - p_{j,\gamma})\right) + k^j_{d,z}\text{sat}_{\sigma^j_{d,z}}\left((R_{n_\gamma}e_3)^T v_j\right) \end{bmatrix} + \\ - m_j R_{n_\gamma} \begin{bmatrix} 0 \\ d_j\left(k^j_{p,\psi} e_3^T \mathcal{S}(n_\gamma)\, n + k^j_{d,\psi}\text{sat}_{\sigma^j_{d,\psi}}(e_3^T\omega)\right) \\ \text{sat}_{\sigma^j_{i,z}}(k^j_{i,z}\xi_{j,z}) \end{bmatrix} \end{aligned} \tag{48}$$

for some positive saturation constants $\sigma^j_{p,x}, \sigma^j_{d,x}, \sigma^j_{p,y}, \sigma^j_{d,y}, \sigma^j_{p,z}, \sigma^j_{d,z}, \sigma^j_{d,\psi}, \sigma^j_{i,z}$ (for example, $\sigma^j_{p,x}$ corresponds to a saturation on the longitudinal position error of UAV j).

Denote

$$\bar{u}_j := m_j \sqrt{\sum_{l\in\{x,y,z\}} \left(k^j_{p,l}\sigma^j_{p,l} + k^j_{d,l}\sigma^j_{d,l}\right)^2 + d_j\left(k^j_{p,\psi} + k^j_{d,\psi}\sigma^j_{d,\psi}\right)^2 + \left(\sigma^j_{i,z}\right)^2}, \tag{49}$$

and suppose the gains and saturations are chosen such that $\bar{u}_j < \|\hat{u}_{j,\gamma}\|$. Then, it follows that

$$0 < \|\hat{u}_{j,\gamma}\| - \bar{u}_j \leq \|u^{pid}_{j,\gamma}(\cdot)\| \leq \|\hat{u}_{j,\gamma}\| + \bar{u}_j \tag{50}$$

and, as such, the control input required from each UAV is bounded, and, simultaneously, the desired attitude for each UAV given by $\frac{u^{pid}_{j,\gamma}(\cdot)}{\|u^{pid}_{j,\gamma}(\cdot)\|}$ is also well defined.

If, in addition, the integral saturations are chosen big enough, specifically if $\sigma^j_{i,z} > \left|\frac{e_3^T(u_{j,\gamma} - \hat{u}_{j,\gamma})}{m_j}\right|$ for $j \in \{1, 2\}$, then it follows that $u^{pid}_{j,\gamma}(\tilde{z}_\gamma) = u_\gamma \Rightarrow \tilde{Z}_\gamma(\tilde{z}_\gamma, u^{pid}_\gamma(\tilde{z}_\gamma)) = 0_{32}$ for

$$\tilde{z}_\gamma := \begin{bmatrix} \bar{z}_\gamma \\ \xi_{1,z,\gamma} \\ \xi_{2,z,\gamma} \end{bmatrix} := \begin{bmatrix} \bar{z}_\gamma \\ \frac{1}{k^1_{i,z}}(\text{sat}_{\sigma^1_{i,z}})^{-1}\left(\frac{e_3^T(u_{1,\gamma} - \hat{u}_{1,\gamma})}{m_1}\right) \\ \frac{1}{k^2_{i,z}}(\text{sat}_{\sigma^2_{i,z}})^{-1}\left(\frac{e_3^T(u_{2,\gamma} - \hat{u}_{2,\gamma})}{m_2}\right) \end{bmatrix}, \tag{51}$$

that is, $\tilde{z}_\gamma$ above is an equilibrium point under the saturated control law (and it degenerates into (44) when $\text{sat}_{\sigma^1_{i,z}}, \text{sat}_{\sigma^2_{i,z}}$ are the identity functions).

Remark 14: Later in this paper, we perform a linearization of the (closed-loop) vector field

$$\tilde{z} \mapsto \tilde{Z}^{cl}_\gamma(\tilde{z}) := \tilde{Z}_\gamma(\tilde{z}, u^{pid}_{j,\gamma}(\tilde{z})) \tag{52}$$

around the equilibrium point $\tilde{z}_\gamma$ (with $\tilde{Z}_\gamma$, $u^{pid}_{j,\gamma}$, $\tilde{z}_\gamma$ defined in (40b), (48), (51)). Let us then discuss the impact the saturations (in the control law in (48)) have on the linearization. For that purpose, recall the vector field $\bar{Z}$ in (30b) and recall that Z in (8b) is input affine (see Remark 2). For that reason, the $\dot{z}$ part in (30b) is linear w.r.t. (u_1, u_2), while the $\dot{r}_i$ part in (30b) is linear w.r.t. $\frac{u_i}{\|u_i\|}$.

Now, denote $\text{id} : \mathbb{R} \ni x \mapsto x \in \mathbb{R}$ as the identity function, and recall that the control law with saturations (in (48)) degenerates into the control law without saturations (in (43)) when $\text{sat}_\sigma = \text{id}$. For brevity, denote

$$\alpha_j = \text{sat}'\left(\text{sat}^{-1}\left(\frac{\hat{u}_{j,\gamma} - u_{j,\gamma}}{m_j}\right)\right)|_{\text{sat}\equiv\text{sat}_{\sigma^j_{i,z}}}$$

and let $\overset{\text{r.b.}}{\to}$ read as $\overset{\text{replaced by}}{\to}$. It may then be verified that

$$\frac{\partial}{\partial\tilde{z}} u^{pid}_{j,\gamma}(\tilde{z})|_{\tilde{z}=\tilde{z}_\gamma} = \left(\frac{\partial}{\partial\tilde{z}} u^{pid}_{j,\gamma}(\tilde{z}_\gamma)|_{\tilde{z}=\tilde{z}_\gamma}\right)|_{\substack{\text{sat}\overset{\text{r.b.}}{\to}\text{id} \\ k^j_{i,z}\overset{\text{r.b.}}{\to}k^j_{i,z}\alpha_j}}, \tag{53a}$$

which in turn implies that

$$\frac{\partial}{\partial\tilde{z}} \frac{u^{pid}_{j,\gamma}(\tilde{z})}{\|u^{pid}_{j,\gamma}(\tilde{z})\|}|_{\tilde{z}=\tilde{z}_\gamma} = \left(\frac{\partial}{\partial\tilde{z}} \frac{u^{pid}_{j,\gamma}(\tilde{z})}{\|u^{pid}_{j,\gamma}(\tilde{z})\|}|_{\tilde{z}=\tilde{z}_\gamma}\right)|_{\substack{\text{sat}\overset{\text{r.b.}}{\to}\text{id} \\ k^j_{i,z}\overset{\text{r.b.}}{\to}k^j_{i,z}\alpha_j}}. \tag{53b}$$

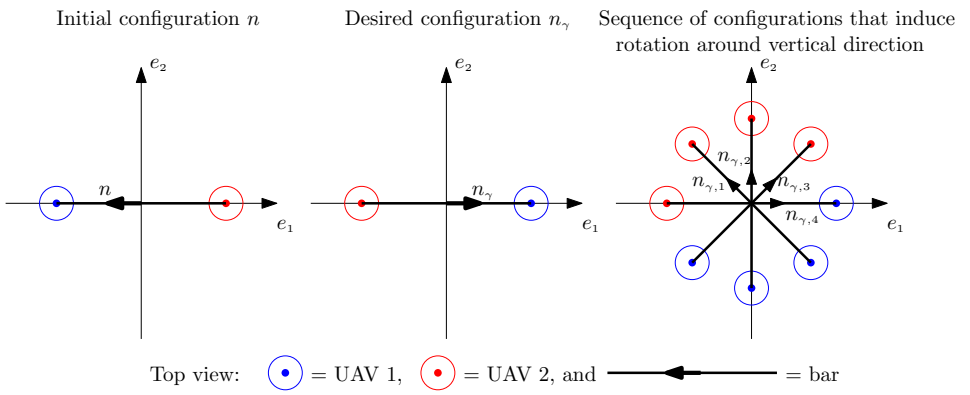

Fig. 8: Create sequence of configurations that induce a rotation of the bar around the vertical direction when the bar is initially (close to) diametrically opposed to the desired configuration.

It follows from (53) that the linearization does not *see* the saturations, provided that the integral gains of the unsaturated control law in (43) are replaced as $k^j_{i,z} \overset{\text{r.b.}}{\to} k^j_{i,z}\alpha_j$, for $j \in 1,2$ (when $\hat{u}_{j,\gamma} = u_{j,\gamma}$, then $k^j_{i,z} \to k^j_{i,z}\text{sat}'(\text{sat}^{-1}(0)) = k^j_{i,z}$, which corresponds to no replacement).

Remark 15: Recall Remark 13, where we established that the closed-loop vector field $\tilde{z} \mapsto \tilde{Z}_\gamma(\tilde{z}, u^{pid}_\gamma(\tilde{z}))$ does not *see* the rotation and offset $(R^T_{n_\gamma}, p_\gamma)$ for the PID control law without saturations in (43). For the PID-control law with saturations in (48) that conclusion no longer holds (the control law is not insensitive to arbitrary translations, owing to the presence of the saturations). However, the results presented later in this paper are of a local nature, and, as we have established in Remark 14, at the equilibrium, the saturated control law in (48) behaves exactly the same way as the unsaturated control law in (43) provided that the integral gains are appropriately scaled.

D. Induce rotations around the vertical axis

As described at the end of Section IV-A, if n is close to $-n_\gamma$, rather than forcing the bar to rotate around the vertical direction, the control law *encourages* the UAVs to swap positions and thus it *encourages* the bar to rotate in the plane spanned by the UAVs. We note that, when the system is restricted to a two-dimensional setting, the bar cannot rotate around the vertical direction, which is however possible in a three-dimensional setting. If n is initially not close enough to n_γ, a possible solution to this problem is to create a sequence $\{n_{\gamma,1}, n_{\gamma,2}, \cdots, n_{\gamma,k}\}$ such that – see Fig. 8: $n_{\gamma,1}$ is close enough to n; $n_{\gamma,k} = n_\gamma$; $n_{\gamma,i+1}$ is closer to n_γ than $n_{\gamma,i}$; and where we only transit to the next point in the sequence $(n_{\gamma,i+1})$ once n is close enough to the previous point $(n_{\gamma,i})$. This problem is mostly one of path planning, which is however not the focus of this manuscript.

V. Conditions for Local Stability

In Section VI, we linearize the closed-loop vector field around the equilibrium, and we verify that the Jacobian is similar to a block triangular matrix, whose block diagonal entries are in controllable form. This section provides immediate tools for the analysis of the eigenvalues of those matrices in controllable form. Denote then, for any $n \in \mathbb{N}$,

$$C_n(a) := \begin{bmatrix} 0 & 1 & 0 & \cdots & 0 \\ 0 & 0 & 1 & \cdots & 0 \\ \vdots & \vdots & \vdots & \ddots & \vdots \\ 0 & 0 & 0 & \cdots & 1 \\ -a_0 & -a_1 & -a_2 & \cdots & -a_{n-1} \end{bmatrix} \in \mathbb{R}^{n\times n} \tag{54}$$

as a matrix in controllable form, and whose eigenvalues are those in $\{\lambda \in \mathbb{C} : \sum_{i=0}^{i=n} a_i\lambda^i = 0\}$. It follows from the Routh's criterion that

$$C_3((a_0,a_1,a_2)) \text{ Hurwitz} \Leftrightarrow a_0,a_1,a_2 > 0 \wedge a_0 < a_1a_2, \tag{55}$$

which we make use of later on. In what follows, denote $q \in \mathbb{R}$, $f := (f_p, f_d) \in (\mathbb{R}_{\geq 0})^2$, $k := (k_p, k_d) \in (\mathbb{R}_{\geq 0})^2$, where, in later sections, q and f provide physical constants of interest, and k provides the controller gains (in particular a proportional and a derivative gain). There are two matrices (in controllable form) that appear several times in Section VI, and therefore we introduce them here. Specifically, we define Γ_3 and Γ_5 as

$$\Gamma_3(f,k) := C_3((f_d(k_p+f_p), f_dk_d+f_p, f_d)), \tag{56a}$$

$$\Gamma_5(q,f,k) := C_5(b_1+b_2)|_{\substack{b_1 \equiv f_d(f_pk_p, f_pk_d, k_p, k_d, 1) \\ b_2 \equiv f_p(1+q)(0,0,f_d,1,0)}}. \tag{56b}$$

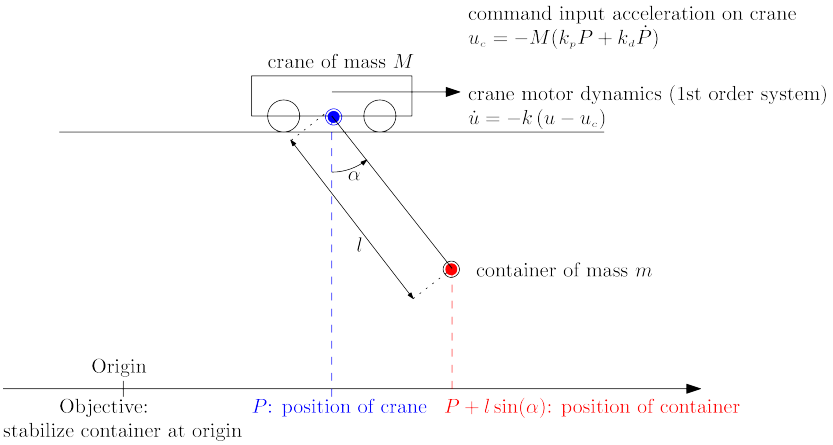

Fig. 9: Container crane system, where crane motor has the dynamics of a first order system. Tethered transportation of a bar can be decomposed in three motions that have similar dynamics to those of a container crane system.

Since we are interested in determining the stability of an equilibrium, it proves useful to determine when a matrix is Hurwitz. That is the case iff all the elements in the first column of the Routh's table are positive (or negative) [37] (these columns are found in the Mathematica notebook file). It follows from the Routh's criterion that (56a) and (56b) are Hurwitz if and only if

$$q > 0 \text{ and } f_d > \frac{k_p}{k_d}. \tag{57}$$

We also define Γ_4 and $\tilde{\Gamma}_4$ as

$$\tilde{\Gamma}_4(\tilde{q}, q, f_p, k) := C_4((f_p(k_p + f_p q\tilde{q}), f_p k_d, k_p + f_p(1+q), k_d)), \tag{58a}$$
$$\Gamma_4(q, f_p, k) := \tilde{\Gamma}_4(0, q, f_p, k), \tag{58b}$$

and it follows from the Routh's criterion that (58b) is Hurwitz iff $q > 0$, and that (58a) is Hurwitz if

$$q(1-\tilde{q}) > 0 \text{ and } k_p > f_p \max(-q, -q\tilde{q}) = -f_p q\tilde{q}. \tag{58c}$$

A. Crane system

As we will verify in the next Section, the tethered transportation of a bar can decomposed in three motions[12] that have similar dynamics to those of a container-crane system. Let us then give some intuition for the results that follow by considering the container-crane system, as illustrated in Fig. 9, where the goal is to stabilize the position of the container at the origin. The dynamics of this system are found in Mathematica notebook files, which are derived by means of the Lagrangian formalism. Under the control law shown in Fig. 9, one obtains a closed loop state matrix

$$A := \begin{bmatrix} 0 & 0 & 1 & 0 & 0 \\ 0 & 0 & 0 & 1 & 0 \\ 0 & g\frac{m}{M} & 0 & 0 & \frac{1}{M} \\ 0 & -\frac{g}{l}\frac{m+M}{M} & 0 & 0 & -\frac{1}{lM} \\ -kk_pM & 0 & -kk_dM & 0 & -k \end{bmatrix} \in \mathbb{R}^{5\times 5}. \tag{59}$$

However, A is not in a form that allows for easily checking the location of its eigenvalues (their location w.r.t. to the imaginary axis, to be more precise). This motivates the introduction of a similarity transformation, namely

$$P := \begin{bmatrix} p & Ap & A^2p & A^3p & A^4p \end{bmatrix} \in \mathbb{R}^{5\times 5}, \text{ with} \tag{60a}$$
$$p := e_1 + le_2 \in \mathbb{R}^5, \tag{60b}$$

where $\det(P) = -\frac{g^3}{lM} \neq 0$. It then follows that (recall Γ_5 in (56b))

$$\bar{A} = PAP^{-1} = \Gamma_5\left(q, (f_p, f_d), (k_p, k_v)\right), \tag{61}$$

where

$$f_p = \frac{g}{l}, f_d = k, \text{ and } q = \frac{m}{M} > 0. \tag{62}$$

[12]When $F_\gamma = 0$ and $e_3^T n_\gamma = 0$.

Notice that f_p is the (squared) frequency of the pendulum, f_d is the gain/frequency of the motor, and q is the ratio between the container's and the crane's masses. If follows from (57), that if

$$k > \frac{k_p}{k_d} \Leftrightarrow \text{motor gain} > \frac{\text{proportional gain}}{\text{derivative gain}}, \tag{63}$$

then $\bar{A} = PAP^{-1}$, and therefore A, is Hurwitz. In other words, if the motor is *fast enough* (the precise meaning is encoded in the inequality above), the container is stabilized around the origin, under the control law shown in Fig 9. One can also provide an interpretation for the similarity matrix P in (60a): it implies that, for the linearized motion, the position of the container, i.e., p as defined in (60b), behaves as a fifth order integrator, i.e.,

$$p^{(5)}(t) = \bar{A}_{5,1}p^{(0)}(t) + \cdots + \bar{A}_{5,5}p^{(4)}(t). \tag{64}$$

Studying the stability of this motion is equivalent to studying the location of the roots of the characteristic polynomial, i.e., $\{s \in \mathbb{C} : s^5 = \bar{A}_{5,1}s^0 + \cdots + \bar{A}_{5,5}s^4\}$, which justifies the results presented in Section V.

VI. Stability Analysis of the Closed-loop System

A. Linearization around point in a manifold

Before linearizing the closed-loop vector field $\tilde{Z}_\gamma^{cl}$ in (52) around the equilibrium $\tilde{z}_\gamma$ in (51), let us provide a vector field that serves only the purpose of analysis.

For that purpose, consider then the constraints, the state space and the vector field

$$f : \mathbb{R}^n \ni y \mapsto f(y) \in \mathbb{R}^m, \tag{65a}$$

$$\mathbb{Y} := \{y \in \mathbb{R}^n : f(y) = 0_m\}, \tag{65b}$$

$$Y : \mathbb{Y} \ni y \mapsto Y(y) \in T_y\mathbb{Y}, \tag{65c}$$

and suppose that the vector field Y vanishes at $y^\star \in \mathbb{Y}$, i.e., $Y(y^\star) = 0_n$. The constraints' map f above is assumed smooth, and, since $Y(y) \in T_y\mathbb{Y}$, it is the case that $Df(y)Y(y) = 0_m$ for all $y \in \mathbb{Y}$. Finally, we assume that $Df(y^\star) \in \mathbb{R}^{m\times n}$ is full rank.

If one linearizes Y around $y^\star$, the resulting Jacobian has m poles that need to be ignored, as these correspond to eigenvalues in directions the system will never exploit. For that purpose, consider then, for any $y \in \mathbb{R}^n$ and for some $\lambda > 0$,

$$Y^\star(y) := Y(y) - Df(y^\star)^T \left(Df(y^\star)Df(y^\star)^T\right)^{-1} \left(Df(y)Y(y) + \lambda f(y)\right), \tag{66}$$

(the inverse above is well defined since $Df(y^\star)$ is full rank) where it follows from (65), that for any $y \in \mathbb{Y}$, $Y^\star(y) = Y(y)$. As such, the vector field $Y^\star$ and Y yield the same trajectories provided that a trajectory starts in $\mathbb{Y}$, and which proves the following result.

Proposition 16: Let Y be a vector field in $\mathbb{Y}$, as defined in (65), and with $y^\star \in \mathbb{Y}$ as an equilibrium point (e.q.). Then, $y^\star$ is an exponentially stable e.q. of Y if and only if $y^\star$ is an exponentially stable e.q. of $Y^\star$, as defined in (66).

Linearizing $Y^\star$ around $y^\star$ yields the Jacobian $DY^\star(y^\star)$ (which is not necessarily the same as the Jacobian $DY(y^\star)$ obtained by linearizing Y around $y^\star$), which is given by

$$\begin{aligned} DY^\star(y^\star) &= \left(\underbrace{\left(I_n - P_\perp^T \left(P_\perp P_\perp^T\right)^{-1} P_\perp\right)}_{=:\Pi_{P_\perp} \in \mathbb{R}^{n\times n}} DY(y^\star) - \lambda P_\perp^T \left(P_\perp P_\perp^T\right)^{-1} P_\perp \right) |_{P_\perp = Df(y^\star)} \\ &= \left(I_n - Df(y^\star)^T \left(Df(y^\star)Df(y^\star)^T\right)^{-1} Df(y^\star)\right) DY(y^\star) - \lambda Df(y^\star)^T \left(Df(y^\star)Df(y^\star)^T\right)^{-1} Df(y^\star), \end{aligned}$$

where we have used the fact that $Y(y_\star) = 0_n$, and where the matrix $\Pi_{P_\perp}$ corresponds to a projection onto the space orthogonal to the directions spanned by $P_\perp^T = Df(y^\star)^T \in \mathbb{R}^{n\times m}$. The purpose of $Y^\star$ is now clear: the m poles of the Jacobian $DY(y^\star)$ associated to the directions spanned by $Df(y^\star)^T$ have been replaced by m poles at $-\lambda < 0$. Indeed, let

$$P := \begin{bmatrix} P_1 \\ P_\perp \end{bmatrix} := \begin{bmatrix} P_1 \\ Df(y^\star) \end{bmatrix} \in \mathbb{R}^{n\times n} \tag{67a}$$

be some change of basis matrix with $P_1 \in \mathbb{R}^{(n-m)\times n}$ (that is, P_1 and $P_\perp := Df(y^\star)$ span $\mathbb{R}^n$), and denote

$$P^{-1} \equiv Q \Leftrightarrow \left(\begin{bmatrix} P_1 \\ P_\perp \end{bmatrix}\right)^{-1} \equiv \begin{bmatrix} Q_1 & Q_2 \end{bmatrix}, \tag{67b}$$

which implies that

$$PP^{-1} = I_n \Leftrightarrow \begin{bmatrix} P_1Q_1 & P_1Q_2 \\ P_\perp Q_1 & P_\perp Q_2 \end{bmatrix} = \begin{bmatrix} I_{n-m} & 0_{(n-m)\times m} \\ 0_{m\times(n-m)} & I_m \end{bmatrix}, \tag{67c}$$

$$P^{-1}P = I_n \Leftrightarrow Q_1P_1 + Q_2P_\perp = I_n. \tag{67d}$$

It then follows that the Jacobian $DY^\star(y^\star)$ is similar to an upper block triangular matrix, specifically

$$PDY^\star(y^\star)P^{-1} = \begin{bmatrix} P_1\Pi_{P_\perp}DY(y^\star)Q_1 & \star_{(n-m)\times m} \\ 0_{m\times(n-m)} & -\lambda I_m \end{bmatrix}|_{P_\perp = Df(y^\star)} \tag{68}$$

$$= \begin{bmatrix} P_1\Pi_{P_\perp}DY(y^\star)\Pi_{P_\perp}Q_1 & \star_{(n-m)\times m} \\ 0_{m\times(n-m)} & -\lambda I_m \end{bmatrix}|_{P_\perp = Df(y^\star)}, \tag{69}$$

i.e, the m poles of the Jacobian $DY(y^\star)$ associated to the directions spanned by $P_\perp = Df(y^\star)^T$ have been replaced by m poles at $-\lambda < 0$ (these are the directions along which the system will never move, since the state space in (65b) is invariant).

Proof of (69)*:* For brevity, let $A \equiv DY(y^\star)$. Then, PAP^{-1} is equivalently expressed as

$$\begin{bmatrix} P_1 \\ P_\perp \end{bmatrix}\left(\Pi_{P_\perp}A - \lambda P_\perp^T\left(P_\perp P_\perp^T\right)^{-1}P_\perp\right)\left(\begin{bmatrix} P_1 \\ P_\perp \end{bmatrix}\right)^{-1} =$$

$$\overset{(67b)}{=} \begin{bmatrix} P_1 \\ P_\perp \end{bmatrix}\left(\Pi_{P_\perp}A - \lambda P_\perp^T\left(P_\perp P_\perp^T\right)^{-1}P_\perp\right)\begin{bmatrix} Q_1 & Q_2 \end{bmatrix}$$

$$\overset{(67c):\, P_\perp Q_1 = 0 \text{ and } P_\perp Q_2 = I}{=} \begin{bmatrix} P_1 \\ P_\perp \end{bmatrix}\begin{bmatrix} \Pi_{P_\perp}AQ_1 & \Pi_{P_\perp}AQ_2 - \lambda P_\perp^T\left(P_\perp P_\perp^T\right)^{-1} \end{bmatrix}$$

$$\overset{P_\perp \Pi_{P_\perp} = 0}{=} \begin{bmatrix} P_1\Pi_{P_\perp}AQ_1 & P_1\Pi_{P_\perp}AQ_2 - \lambda P_1 P_\perp^T\left(P_\perp P_\perp^T\right)^{-1} \\ 0_{m\times(n-m)} & -\lambda I_m \end{bmatrix}$$

$$\overset{(67c):\, P_\perp Q_1 = 0 \Rightarrow Q_1 = \Pi_{P_\perp}Q_1}{=} \begin{bmatrix} P_1\Pi_{P_\perp}A\Pi_{P_\perp}Q_1 & P_1\Pi_{P_\perp}AQ_2 - \lambda P_1 P_\perp^T\left(P_\perp P_\perp^T\right)^{-1} \\ 0_{m\times(n-m)} & -\lambda I_m \end{bmatrix}.$$

■

Remark 17: It is now clear from (66) why we needed to provide the constraint maps f, $\bar{f}$ and $\tilde{f}$ defined in (5), (29), (39).

Remark 18: Let us describe one possible way of computing Q_1 in $P^{-1} \equiv Q = \begin{bmatrix} Q_1 & Q_2 \end{bmatrix}$, without needing to compute the complete inverse P^{-1} (this method is not necessarily better than computing the whole P^{-1}). For that purpose, given a matrix $B \in \mathbb{R}^{(n-m)\times n}$, denote $B^\perp \in \mathbb{R}^{n\times m}$ as any matrix that spans the null space of B (i.e., $BB^\perp = 0_{(n-m)\times m}$ and $\text{rank}\left(\begin{bmatrix} B^T & B^\perp \end{bmatrix}\right) = n$). Then, it follows that

$$P^{-1} \equiv Q \Leftrightarrow \left(\begin{bmatrix} P_1 \\ P_\perp \end{bmatrix}\right)^{-1} \equiv \begin{bmatrix} Q_1 & Q_2 \end{bmatrix} \text{ with} \tag{70a}$$

$$\begin{bmatrix} Q_1 & Q_2 \end{bmatrix} := \begin{bmatrix} (I_n - P_1^\perp(P_\perp P_1^\perp)^{-1}P_\perp)P_1^T(P_1P_1^T)^{-1} & (I_n - P_\perp^\perp(P_1P_\perp^\perp)^{-1}P_1)P_\perp^T(P_\perp P_\perp^T)^{-1} \end{bmatrix} \in \mathbb{R}^{n\times n} \tag{70b}$$

is the inverse of P. Verifying that

$$PP^{-1} = I_n \Leftrightarrow \begin{bmatrix} P_1Q_1 & P_1Q_2 \\ P_\perp Q_1 & P_\perp Q_2 \end{bmatrix} = \begin{bmatrix} I_{n-m} & 0_{(n-m)\times m} \\ 0_{m\times(n-m)} & I_m \end{bmatrix} \tag{70c}$$

is simple. Verifying that

$$P^{-1}P = I_n \Leftrightarrow Q_1P_1 + Q_2P_\perp = I_n \tag{70d}$$

may be accomplished by using the singular-value decomposition of P ($UDV^T = \begin{bmatrix} P_1 \\ P_\perp \end{bmatrix}$ and $VD^{-1}U^T = \begin{bmatrix} P_\perp^\perp & P_1^\perp \end{bmatrix}$ for some unitary matrices U, V and some invertible diagonal matrix D). Finally, we emphasize that (70b) is independent of the choice of $P_i^\perp$ (i.e., any choice of matrix $P_i^\perp$ yields the same result; that is the case because, given two distinct $(P_1^\perp)^A$ and $(P_1^\perp)^B$, they are always related in that $(P_1^\perp)^A = (P_1^\perp)^B C$ for some invertible $C \in \mathbb{R}^{m\times m}$; and, therefore, $(P_1^\perp)^A(P_\perp(P_1^\perp)^A)^{-1} = (P_1^\perp)^B C(P_\perp(P_1^\perp)^A C)^{-1} = (P_1^\perp)^B(P_\perp(P_1^\perp)^B)^{-1}$).

B. Linearization of the closed-loop vector field

Recall now the closed-loop vector field $\tilde{Z}_\gamma^{cl}$ in (52) around the equilibrium $\tilde{z}_\gamma$ in (51). Recall also Remark 15, where we concluded that it suffices to study $\gamma_\star$ (instead of γ). Given that the motion of our system is constrained in a manifold and for the reasons described in the previous section, we modify the vector field as in (66) (this change serves only the purpose of analysis). We then compute the Jacobian

$$A := D(\tilde{Z}_\gamma^{cl})^\star(\tilde{z}_\gamma) \in \mathbb{R}^{32\times 32} (\text{with } (\tilde{Z}_\gamma^{cl})^\star \text{ as defined in (66)}), \tag{71}$$

which is sparse, but unstructured (in (71), $Y \equiv \tilde{Z}_{\gamma_\star}^{cl}$, and $Y^\star \equiv (\tilde{Z}_{\gamma_\star}^{cl})^\star$, with $Y^\star$ as defined in (66)). Moreover, the Jacobian is neither a diagonal nor a triangular matrix, and thus determining whether it is Hurwitz is not straightforward. For that purpose, we provide a similarity matrix, i.e., $P \in \mathbb{R}^{32\times 32}$, such that PAP^{-1} is a block triangular matrix, and where each block diagonal

Under-actuated UAVS		Fully-actuated UAVs and no integral action	
Symmetric	Non-symmetric	Symmetric	Symmetric
$(\theta_\star, F_\star) = (0, 0)$		$\theta_\star \neq 0$ and $F_\star = 0$	$\theta_\star = 0$ and $F_\star \neq 0$
Section VI-C	Section VI-D	Section VI-E	Section VI-F

TABLE I: Analysis of stability of equilibrium is performed for different scenarios (symmetric system is illustrated in Fig. 1a and asymmetric system is illustrated in Fig. 1b).

matrix is in controllable form (allowing us to invoke the results from Section V). To be specific, we provide a change of basis matrix

$$P := \begin{bmatrix} P_1 & \cdots & P_k & P_\perp \end{bmatrix}^T, \tag{72a}$$

for some $k \in \mathbb{N}$, such that PAP^{-1} is a block triangular matrix, i.e.,

$$PAP^{-1} = \begin{bmatrix} A_1 \oplus \cdots \oplus A_k & \star \\ 0 & -\lambda I \end{bmatrix}. \tag{72b}$$

That is, we provide a change of basis that breaks the motion of the system into k decoupled motions (note that the $\lambda > 0$ in (72b) is that chosen in (66)). Thus $\text{eig}(A) = \{-\lambda\} \cup \text{eig}(A_1) \cup \ldots \cup \text{eig}(A_k)$, and, therefore, determining whether the Jacobian A in (71) is Hurwitz amounts to checking whether each of the blocks in (72b) is Hurwitz.

Recall Remark 13, where we established that there are *truly* only two equilibrium parameters that need to be studied, namely the desired normal force to be exerted on the bar $F_\star$ and the desired pitch angle of the bar $\theta_\star$. In the next four subsections, we analyze four separate cases, as listed in Table I. Analyzing the most generic of cases (one where the system is not symmetric, the pitch is non-zero, and the normal force is also non-zero) is left for future research.

C. Symmetric UAVs-bar system

Let us discuss first the case where the system UAVs-bar is symmetric, i.e., when the cables have the same length; when the contacts points on the bar are at the same distance from the bar's center-of-mass (but in opposite directions); and, when the UAVs are identical, with the same weight and the same control law gains. This can be described as

$$\begin{cases} l_1 = l_2 =: l > 0 \\ d_1 = -d_2 =: d \in \mathbb{R} \\ m_1 = m_2 =: M > 0 \\ k^1_{l,h} = k^2_{l,h} =: k_{l,h} > 0 \text{ for } l \in \{p, i, d\} \text{ and } h \in \{x, y, \mathrm{z}\} \\ k^1_r = k^2_r =: k_r > 0 \end{cases} \tag{73}$$

and where we let $k^j_{p,\psi} = 0$ and $k^j_{d,\psi} = 0$ for $j \in \{1, 2\}$. This case provides us with intuition on how to decompose the Jacobian into three decoupled motions (vertical, longitudinal and lateral), and it is basis for the generic case where the system does not satisfy the symmetry conditions in (73).

Consider then the similarity matrix

$$P := \begin{bmatrix} P_z & P_\theta & P_x & P_\delta & P_y & P_\psi & P_\perp \end{bmatrix}^T \in \mathbb{R}^{32\times 32}, \tag{74a}$$

where (below A is the Jacobian in (71), and $e_1, \cdots, e_{32}$ are the canonical basis vectors in $\mathbb{R}^{32}$)

$$P_z := \begin{bmatrix} \nu & A\nu & A^2\nu \end{bmatrix}\big|_{\nu = \frac{d_2 e_{31} - d_1 e_{32}}{d_2 - d_1}} \in \mathbb{R}^{32\times 3}, \tag{74b}$$

$$P_\theta := \begin{bmatrix} \nu & A\nu & A^2\nu \end{bmatrix}\big|_{\nu = \frac{e_{31} - e_{32}}{d_2 - d_1}} \in \mathbb{R}^{32\times 3}, \tag{74c}$$

$$P_x := \begin{bmatrix} e_1 & Ae_1 & A^2e_1 & A^3e_1 & A^4e_1 \end{bmatrix} \in \mathbb{R}^{32\times 5}, \tag{74d}$$

$$P_\delta := \begin{bmatrix} \nu & A\nu & A^2\nu \end{bmatrix}\big|_{\nu = e_7 - e_{10}} \in \mathbb{R}^{32\times 3}, \tag{74e}$$

$$P_y := \begin{bmatrix} e_2 & Ae_2 & A^2e_2 & A^3e_2 & A^4e_2 \end{bmatrix} \in \mathbb{R}^{32\times 5}, \tag{74f}$$

$$P_\psi := \begin{bmatrix} e_5 & Ae_5 & A^2e_5 & A^3e_5 & A^4e_5 \end{bmatrix} \in \mathbb{R}^{32\times 5}, \tag{74g}$$

and, finally, where $P_\perp := (D\tilde{f}(\tilde{z}_\gamma))^T \in \mathbb{R}^{32\times 8}$ (where $\tilde{f}$ is the constraints map defined in (39b)). Note that $|P| = -\frac{d^3 g^{13} m^3 (m+2M)^4}{4J^3 L^{13} M^4}$ which is non-zero provided that $d \neq 0$ (when $d_1 = -d_2 = d = 0$, the bar's angular velocity is constant and equal to its initial condition, which implies the bar's angular position is uncontrollable – this agrees with intuition).

Remark 19: Recall the state decomposition in (39a) (which builds upon (29a) and (2)), and that $\dot{\tilde{z}} = A\tilde{z}$, for the linearized motion around the equilibrium. Then (for brevity, denote $p = (x, y, \mathtt{z})$ and $n = (\cdot, \psi, \theta)$)

$$\begin{bmatrix} P_x^T z \\ P_\delta^T z \\ P_y^T z \\ P_\psi^T z \end{bmatrix} = \begin{bmatrix} (x^{(0)}, x^{(1)}, x^{(2)}, x^{(3)}, x^{(4)}) \\ (\delta^{(0)}, \delta^{(1)}, \delta^{(2)})|_{\delta = e_1^T(p_1 - p_2)} \\ (y^{(0)}, y^{(1)}, y^{(2)}, y^{(3)}, y^{(4)}) \\ (\psi^{(0)}, \psi^{(1)}, \psi^{(2)}, \psi^{(3)}, \psi^{(4)}) \end{bmatrix}, \tag{75}$$

and (the equalities below can only be verified under an appropriate coordinate transformation – see Mathematica notebook file or [31])

$$\begin{bmatrix} P_{\mathtt{z}}^T z \\ P_\theta^T z \end{bmatrix} = \begin{bmatrix} (\mathtt{z}^{(-1)}, \mathtt{z}^{(0)}, \mathtt{z}^{(1)}) \\ (\theta^{(-1)}, \theta^{(0)}, \theta^{(1)}) \end{bmatrix}. \tag{76}$$

That is, P_x is associated with the longitudinal (x) linear motion of the bar (fifth order system) and P_δ is associated with the longitudinal linear motion between the UAVs (third order system); P_y is associated with the lateral (y) linear motion of the bar (fifth order system) and P_ψ is associated with the lateral angular motion of bar (fifth order system). And finally, $P_{\mathtt{z}}$ is associated with the vertical ($\mathtt{z}$) linear motion of the bar (third order system) and P_θ is associated with the vertical angular motion of the bar (third order system): to be specific, the sum of the integral errors is associated with the vertical linear position of the bar, and the difference is associated with the vertical angular position of the bar.

Given the state matrix A in (71) and the similarity matrix P in (74a), it then follows that

$$PAP^{-1} = \begin{bmatrix} A_{\mathtt{z}} \oplus A_\theta \oplus A_x \oplus A_\delta \oplus A_y \oplus A_\psi & \star \\ 0_{8\times 24} & -\lambda I_{8\times 8} \end{bmatrix} \in \mathbb{R}^{32\times 32}, \tag{77}$$

where (77) is a block triangular matrix, with the first block as a block diagonal matrix with six blocks (note that the λ in (77) is that chosen in (66)). Thus $\mathrm{eig}(A) = \{-\lambda\} \cup \mathrm{eig}(A_{\mathtt{z}}) \cup \mathrm{eig}(A_\theta) \cup \mathrm{eig}(A_x) \cup \mathrm{eig}(A_\delta) \cup \mathrm{eig}(A_y) \cup \mathrm{eig}(A_\psi)$, and, therefore, determining whether the Jacobian A in (71) is Hurwitz amounts to checking whether each of the six blocks in (77) is Hurwitz.

Recall now the definitions in Section V, namely (55) and (56a)–(56b).

1) Longitudinal motion: The matrices A_x and A_δ describe the linear and angular longitudinal motions, and they are given by

$$A_x = \Gamma_5(q, f, k)\,|_{q=\frac{m}{2M},(f_p,f_d)=(\frac{g}{l},k_r),k=(k_{p,x},k_{d,x})}, \tag{78a}$$

$$A_\delta = \Gamma_3(f, k)\,|_{f=(\frac{g}{l}\frac{m}{2M},k_r),k=(k_{p,x},k_{d,x})}, \tag{78b}$$

which are both Hurwitz provided that (see (57))

$$k_r > \frac{k_{p,x}}{k_{d,x}}. \tag{78c}$$

i.e., provided that the attitude inner loop gain is big enough. Since $P_x z = e_1^T p =: x$ and $P_\delta z = e_1^T(p_1 - p_2) =: \delta$, it follows from (78a) and (78b) that, for the linearized motion, the bar's x-position behaves as a fifth-order integrator and the longitudinal displacement between UAVs behaves as a third-order integrator, i.e.,

$$x^{(5)}(t) = (A_x)_{5,5}x^{(4)}(t) + \cdots + (A_x)_{5,1}x^{(0)}(t), \tag{78d}$$

$$\delta^{(3)}(t) = (A_\delta)_{3,3}\delta^{(2)}(t) + \cdots + (A_\delta)_{3,1}\delta^{(0)}(t). \tag{78e}$$

Remark 20: Recall the crane system results presented in Section V-A. It follows that the linearized longitudinal (x) linear motion of the bar is exactly that of the container in a container-crane system, with a cable of length l, being pulled by a crane of mass $2M$, and with a motor constant k_r – see Section V-A.

2) Lateral motion: The matrices A_y and A_ψ describe the linear and angular lateral motions, and they are given by

$$A_y = \Gamma_5(q, f, k)\,|_{q=\frac{m}{2M},(f_p,f_d)=(\frac{g}{l},k_r),k=(k_{p,y},k_{d,y})}, \tag{79a}$$

$$A_\psi = \Gamma_5(q, f, k)\,|_{q=\frac{J}{d^2m}\frac{m}{2M},(f_p,f_d)=(\frac{d^2m}{J}\frac{g}{l},k_r),k=(k_{p,y},k_{d,y})}, \tag{79b}$$

which are both Hurwitz provided that (see (57))

$$k_r > \frac{k_{p,y}}{k_{d,y}}, \tag{79c}$$

i.e., provided that the attitude inner loop gain is big enough. Since $P_y z = e_2^T p =: y$ and $P_\psi z = e_2^T n =: \psi$, it follows from (79a) and (79b) that, for the linearized motion, the bar's lateral linear motion and the bar's lateral angular motion behave as fifth-order integrators, i.e.,

$$y^{(5)}(t) = (A_y)_{5,5}y^{(4)}(t) + \cdots + (A_y)_{5,1}y^{(0)}(t), \tag{79d}$$

$$\psi^{(5)}(t) = (A_\psi)_{5,5}\psi^{(4)}(t) + \cdots + (A_\psi)_{5,1}\psi^{(0)}(t). \tag{79e}$$

Remark 21: A similar remark to Remark 20 can be made at this point, regarding the lateral motions.

3) Vertical motion: The matrices A_{z} and A_θ describe the linear and angular vertical motions, and they are given by

$$A_{\mathrm{z}} = C_3(\gamma_{\mathrm{z}}(k_{i,\mathrm{z}}, k_{p,\mathrm{z}}, k_{d,\mathrm{z}})), \text{ with } \gamma_{\mathrm{z}} = \left(1 + \frac{m}{2M}\right)^{-1}, \tag{80a}$$

$$A_\theta = C_3(\gamma_\theta(k_{i,\mathrm{z}}, k_{p,\mathrm{z}}, k_{d,\mathrm{z}})), \text{ with } \gamma_\theta = \left(1 + \frac{J}{d^2 m}\frac{m}{2M}\right)^{-1}, \tag{80b}$$

which are Hurwtiz provided that (see (55))

$$k_{i,\mathrm{z}} < \min(\gamma_{\mathrm{z}}, \gamma_\theta) k_{p,\mathrm{z}} k_{d,\mathrm{z}}. \tag{80c}$$

i.e., provided that the integral gain is *small enough*. Note that, for a regular PID (where $\dot{x} = C_3(-(k_i, k_p, k_d))x$), it is required that $k_{i,\mathrm{z}} < k_{p,\mathrm{z}} k_{d,\mathrm{z}}$, while the constraint above is more restrictive, since $\gamma_{\mathrm{z}} < 1$ and $\gamma_\theta < 1$. Moreover, notice that γ_θ vanishes when d vanishes (the distance of the contact points to the bar's center-of-mass): as such, it is advisable to have a *big* d (*big* compared with $\sqrt{\frac{J}{2M}}$), because γ_θ is closer to 1 (and thus the bound on the integral gain is less restrictive). This also agrees with intuition, which suggests that controlling the bar's attitude when the contact points are too close to the bar's center-of-mass is difficult. Under an appropriate coordinate change (see the Mathematica notebook file or [31], it can be verified that the sum of the integral errors is related to the vertical linear position of the bar (i.e., if $\mathrm{z}^{(-1)} \equiv \frac{d_2\xi_{1,\mathrm{z}} - d_1\xi_{2,\mathrm{z}}}{d_2 - d_1}$ then $\mathrm{z}^{(1)} \equiv \frac{d^2}{dt^2}\frac{d_2\xi_{1,\mathrm{z}} - d_1\xi_{2,\mathrm{z}}}{d_2 - d_1} = v_{\mathrm{z}}$), while the difference between the integral errors is related to the vertical angular position of the bar (i.e., if $\theta^{(-1)} \equiv \frac{\xi_{1,\mathrm{z}} - \xi_{2,\mathrm{z}}}{d_2 - d_1}$ then $\theta^{(1)} \equiv \frac{d^2}{dt^2}\frac{\xi_{1,\mathrm{z}} - \xi_{2,\mathrm{z}}}{d_2 - d_1} = \omega_y$). As such, for the linearized motion,

$$\mathrm{z}^{(2)}(t) = (A_{\mathrm{z}})_{3,3}\mathrm{z}^{(1)}(t) + (A_{\mathrm{z}})_{3,2}\mathrm{z}^{(0)}(t) + (A_{\mathrm{z}})_{3,1}\mathrm{z}^{(-1)}(t), \tag{80d}$$

$$\theta^{(2)}(t) = (A_\theta)_{3,3}\theta^{(1)}(t) + (A_\theta)_{3,2}\theta^{(0)}(t) + (A_\theta)_{3,1}\theta^{(-1)}(t). \tag{80e}$$

Remark 22: We also emphasize that, for the linearized motion, and for $i \in \{x, y, \mathrm{z}\}$, the proportional and derivative gains $k_{p,i}$ and $k_{d,i}$ have an effect on the i-motion only, which agrees with intuition. This is however not the case when the bar is required to be under normal stress ($F_\star \neq 0$) nor when the bar is required to have a non-zero pitch ($\theta_\star \neq 0$) – see Sections VI-E and VI-F.

Remark 23: The attitude gains of the vehicles do not play a role in the linearized vertical motion.

At this point, we defer the presentation of our main result (Theorem 29) till the end on the next subsection, which considers the generic case where the system is asymmetric.

D. Non-symmetric UAVs-bar system

Let us now consider the case where the system is not symmetric, i.e., a system which does not satisfy the conditions in (73) (we assume only that d_1, d_2 have opposite signs – see Remark 3). The idea will be to choose the UAVs' gains so as to compensate for the asymmetries, in such a way that if the system degenerates into a symmetric one, then the results of the previous section are recovered.

Consider again the similarity matrix $P \in \mathbb{R}^{32\times 32}$ as defined in (74a) (which will be different than the P obtained in the previous section, which relied on the symmetry conditions), whose determinant is given by

$$|P| = 2^5 g^2 \left(\frac{g}{l_1 l_2 (d_1 - d_2)}\right)^8 \left(\frac{g(d_1 d_2 m)(d_1 l_1 - d_2 l_2)}{J(d_1 - d_2)}\right)^3 \left(d_1 - d_2\left(\frac{m}{m_1} + 1\right)\right)^2 \left(d_2 - d_1\left(\frac{m}{m_2} + 1\right)\right)^2 \tag{81}$$

which is non-zero since d_1 and d_2 have opposite signs.

Given the state matrix A in (71) and the similarity matrix P in (74a), it then follows that

$$PAP^{-1} = \begin{bmatrix} A_{\mathrm{z},\theta} \oplus A_{x,\delta} \oplus A_{y,\psi} & \star \\ 0_{8\times 24} & -\lambda I_{8\times 8} \end{bmatrix} \in \mathbb{R}^{32\times 32}, \tag{82}$$

where (82) is a block triangular matrix, with the first block as a block diagonal matrix with three blocks (note that the λ in (82) is that chosen in (66)). Thus $\mathrm{eig}(A) = \{-\lambda\} \cup \mathrm{eig}(A_{\mathrm{z},\theta}) \cup \mathrm{eig}(A_{x,\delta}) \cup \mathrm{eig}(A_{y,\psi})$, and, therefore, determining whether the Jacobian A in (71) is Hurwitz amounts to checking whether each of the three blocks in (82) is Hurwitz. Let us look at each of these matrices separately, corresponding to three decoupled motions.

Similarly to the symmetric system, described in the previous section, there are three decoupled motions, namely a vertical, a longitudinal and a lateral. However, for the symmetric system, each of those motions was in turn composed of two decoupled sub-motions, one linear and one angular; that is not the case for the asymmetric system. The main idea explored next is to choose the control gains such that the linear sub-motion of the vertical/longitudinal/lateral motion is decoupled from the angular sub-motion. The difference with the case where the system is symmetric lies in the fact that the linear and angular sub-motions are not decoupled. This will produce a state matrix that is similar to a block triangular matrix, which we are still able to analyze.

1) Longitudinal motion: Recall Remark 19, and note that P_x and P_δ are associated to $A_{x,\delta} \in \mathbb{R}^{8\times 8}$ in (82). As such, $A_{x,\delta}$ is associated with the longitudinal motion, namely the longitudinal linear motion of the bar, and the longitudinal angular motion corresponding to the longitudinal relative motion between the two UAVs.

In what follows denote

$$F_x \equiv F_x(k^1_{p,x}, k^2_{p,x}, k^1_{d,x}, k^2_{d,x}, k^1_r, k^2_r) \in \mathbb{R}^3, \tag{83}$$

where F_x is some function of the gains shown above (found in the Mathematica notebook file). Note then that $A_{x,\delta}$ has a specific structure, namely (below $\star$ denotes a vector in $\mathbb{R}^5$)

$$A_{x,\delta} = \begin{bmatrix} A_x & e_5 F_x^T \\ e_3 \star^T & A_\delta \end{bmatrix} \in \mathbb{R}^{(5+3)\times(5+3)}. \tag{84}$$

Notice that $A_{x,\delta}$ can be rendered block triangular, if one chooses the gains such that F_x in (84) vanishes. That is accomplished if, for $j \in \{1,2\}$,

$$\begin{aligned} k^j_{p,x} &= k_{p,x} + \frac{d_j l_j}{d_1 l_1 - d_2 l_2} f_{p,x} \Delta_x, \\ k^j_{d,x} &= k_{d,x} + \frac{d_j l_j}{d_1 l_1 - d_2 l_2} \frac{f_{p,x}}{k_r} \Delta_x, \\ k^1_r &= k^2_r = k_r, \end{aligned} \tag{85a}$$

where

$$\Delta_x = \frac{m(d_1 l_1 m_1 + d_2 l_2 m_2)}{m_1 m_2 (d_1 l_1 - d_2 l_2)}, \tag{85b}$$

for some positive $k_{p,x}$, $k_{d,x}$, and k_r, and where $f_{p,x}$ is that in (87a). That is, the proportional and derivative gains of each vehicle must be the same up to some difference that is proportional to the asymmetry of the system, as quantified by Δ_x. If the vehicles' gains are chosen as above, then

$$A_{x,\delta} = \begin{bmatrix} A_x & 0_{5\times 3} \\ \star_{3\times 5} & A_\delta \end{bmatrix} \in \mathbb{R}^{8\times 8} \tag{86}$$

where (recall Γ_5 in (56b))

$$A_x = \Gamma_5(q, f, k)\,|_{q=q_x, f=(f_{p,x},k_r), k=(k_{p,x},k_{d,x})}, \tag{87a}$$

$$f_{p,x} = \frac{g(l_1+l_2)}{2 l_1 l_2} > 0, q_x = \frac{m(d_1^2 l_1^2 m_1 + d_2^2 l_2^2 m_2)}{m_1 m_2 (d_1 l_1 + d_2 l_2)^2} > 0, \tag{87b}$$

and where (recall Γ_3 in (56a))

$$A_\delta = \Gamma_3(f, k)\,|_{f=(\tilde{f}_{p,x},k_r), k=(k_{p,x},k_{d,x}),\ \tilde{f}_{p,x}=\frac{gm(d_1^2 l_1^2 m_1 + d_2^2 l_2^2 m_2)}{l_1 l_2 m_1 m_2 (d_1-d_2)(d_1 l_1 - d_2 l_2)}}. \tag{87c}$$

It follows from (57) that A_x and A_δ above are Hurwitz, provided that

$$k_r > \frac{k_{p,x}}{k_{d,x}}, \tag{88}$$

i.e., provided that the attitude inner loop gain is big enough. This constraint can be comprehended intuitively: fast tracking along the longitudinal direction requires a fast attitude inner loop.

Remark 24: If one wishes both gains $k^1_{p,x}$ and $k^2_{p,x}$, in (85), to be positive, then one must impose that $k_{p,x} > -f_p \min\left(\frac{d_1 l_1 \Delta_x, d_2 l_2 \Delta_x}{d_1 l_1 - d_2 l_2}\right)$, where Δ_x encapsulates some measure of asymmetry of the system. As illustrated in Fig. 10, there are *good and bad* asymmetries: in *good* asymmetries $\Delta_x = 0$ and, therefore, it is only required that $k_{p,x}$ be positive; and, in *bad* asymmetries $\Delta_x \neq 0$ and, therefore, it is required that $k_{p,x}$ be strictly positive.

Remark 25: Recall Remark 19. It follows from (86) that, for the linearized motion, (denote $X := (x^{(0)}, \cdots, x^{(4)})$ and $\Delta := (\delta^{(0)}, \cdots, \delta^{(2)})$)

$$\begin{bmatrix} \dot{X} \\ \dot{\Delta} \end{bmatrix} = \begin{bmatrix} A_x & 0_{5\times 3} \\ \star_{3\times 5} & A_\delta \end{bmatrix} \begin{bmatrix} X \\ \Delta \end{bmatrix}, \tag{89}$$

i.e., the longitudinal linear motion behaves as a fifth order integrator and decoupled from the longitudinal angular motion; while the longitudinal angular motion behaves as a third order integrator, cascaded after the longitudinal linear motion.

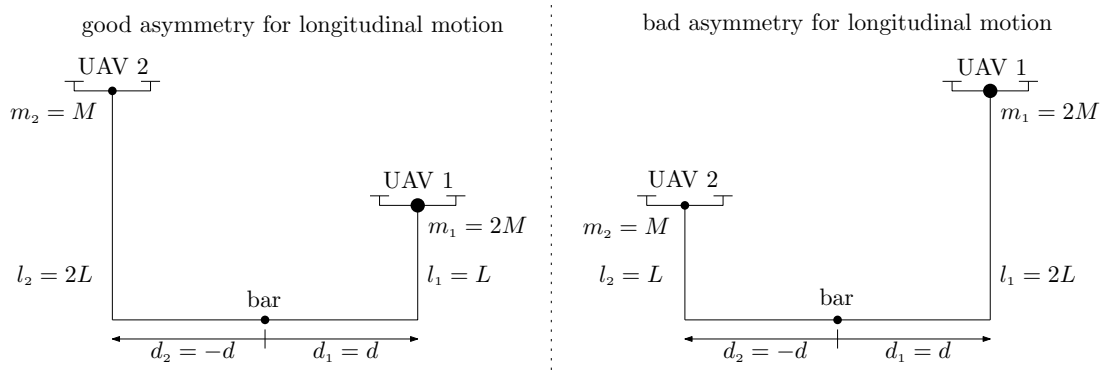

Fig. 10: Good and bad asymmetries: it is better for the heavier UAV to be attached to the shorter cable as it minimizes $|\Delta_x|$. A good asymmetry only requires the gains $k_{p,x}, k_{d,x}$ to be positive, and a bad asymmetry requires both the proportional and the derivative gains to be strictly positive.

2) Lateral motion: Recall Remark 19, and note that P_y and P_ψ are associated to $A_{y,\psi} \in \mathbb{R}^{10\times 10}$ in (82). As such, $A_{y,\psi}$ is associated with the lateral motion, namely the lateral linear motion of the bar, and the lateral angular motion of the bar (yaw motion). In what follows denote

$$F_y \equiv F_y(k^1_{p,y}, k^2_{p,y}, k^1_{d,y}, k^2_{d,y}, k^1_{p,\psi}, k^2_{p,\psi}, k^1_{d,\psi}, k^2_{d,\psi}, k^1_r, k^2_r) \in \mathbb{R}^5, \tag{90}$$

where F_y is some function of the gains shown above (found in the Mathematica notebook file). Note then that $A_{y,\psi}$ has a specific structure, namely

$$A_{y,\psi} = \begin{bmatrix} A_y & e_5 F_y^T \\ e_5 \tilde{F}_y^T & A_\psi \end{bmatrix} \in \mathbb{R}^{(5+5)\times(5+5)}. \tag{91}$$

Notice that $A_{y,\psi}$ can be rendered block triangular, if one chooses the gains such that F_y in (91) vanishes (no choice of gains makes $\tilde{F}_y$ vanish). Indeed, that is accomplished if, for $j \in \{1,2\}$,

$$\begin{aligned}
k^j_{p,y} &= k_{p,y} + \frac{d_j l_j}{d_1 l_1 - d_2 l_2} f_{p,y}\Delta_y, \\
k^j_{d,y} &= k_{d,y} + \frac{d_j l_j}{d_1 l_1 - d_2 l_2} \frac{f_{p,y}}{k_r}\Delta_y, \\
k^j_{p,\psi} &= \frac{d_j l_j}{d_1 - d_2}\left(\frac{d_1 - d_2}{d_1 l_1 - d_2 l_2} f_{p,y}\Delta_y + \frac{l_2 - l_1}{l_1 l_2} k_{p,y}\right), \\
k^j_{d,\psi} &= \frac{d_j l_j}{d_1 - d_2}\left(\frac{d_1 - d_2}{d_1 l_1 - d_2 l_2} \frac{f_{p,y}}{k_r}\Delta_y + \frac{l_2 - l_1}{l_1 l_2} k_{d,y}\right), \\
k^1_r &= k^2_r = k_r,
\end{aligned} \tag{92a}$$

where

$$\Delta_y = \frac{m(d_1 l_1 m_1 + d_2 l_2 m_2)}{m_1 m_2 (d_1 l_1 - d_2 l_2)} + \frac{-m d_1 d_2}{J}\frac{(d_1 - d_2)(l_1 - l_2)}{(d_1 l_1 - d_2 l_2)}, \tag{92b}$$

and for some positive gains $k_{p,y}$ and $k_{d,\psi}$, and where $f_{p,y}$ is that in (93). That is, the proportional and derivative lateral gains of each vehicle must be the same up to some difference that is proportional to the asymmetry of the system, quantified in Δ_y and $|l_2 - l_1|$. If the vehicles' gains are chosen as in (92a), then

$$A_y = \Gamma_5(q, f, k)\,|_{q=q_y, f=(f_{p,y}, k_r), k=(k_{p,y}, k_{d,y})}, \tag{93a}$$

$$A_\psi = \Gamma_5(q, f, k)\,|_{q=q_\psi, f=(f_{p,\psi}, k_r), k=(k_{p,y}, k_{d,y})}, \tag{93b}$$

where (below we assume that d_1 and d_2 have opposite signs)

$$f_{p,y} = \frac{g}{l_1 l_2}\frac{d_1 l_1 - d_2 l_2}{d_1 - d_2} > 0, q_y = \frac{m(d_1^2 l_1^2 m_1 + d_2^2 l_2^2 m_2)}{m_1 m_2 (d_1 l_1 - d_2 l_2)^2} + \frac{-m d_1 d_2}{J}\frac{-d_1 d_2 (l_1 - l_2)^2}{(d_1 l_1 - d_2 l_2)^2} > 0, \tag{93c}$$

$$f_{p,\psi} = \frac{-m d_1 d_2}{J} f_{p,y} > 0, q_\psi = \frac{J}{-m d_1 d_2} q_y > 0, \tag{93d}$$

and which are both Hurwitz provided that

$$k_r > \frac{k_{p,y}}{k_{d,y}}, \tag{94}$$

i.e., provided that the attitude inner loop gain is big enough. Note that similar remarks to Remarks 24 and 25 can be made at this point regarding the lateral motion.

Remark 26: Note that all parameters in (93) are positive, since d_1 and d_2 have opposite signs.

3) Vertical motion: Recall Remark 19, and note that P_z and P_θ are associated to $A_{z,\theta} \in \mathbb{R}^{6\times 6}$ in (82). As such, $A_{z,\theta}$ is associated with the vertical motion, namely the vertical linear motion of the bar, and the vertical angular motion of the bar (pitch motion).

In what follows denote

$$F_z \equiv F_z(k^1_{p,z}, k^2_{p,z}, k^1_{d,z}, k^2_{d,z}, k^1_{i,z}, k^2_{i,z}) \in \mathbb{R}^3, \tag{95}$$

where F_z is some function of the gains shown above (found in the Mathematica notebook file). Note then that $A_{z,\theta}$ has a specific structure, namely

$$A_{z,\theta} = \begin{bmatrix} A_z & e_3 F_z^T \\ e_3 \tilde{F}_z^T & A_\theta \end{bmatrix} \in \mathbb{R}^{(3+3)\times(3+3)}. \tag{96}$$

Notice that $A_{z,\theta}$ can be rendered block triangular, if one chooses the gains such that either F_z or $\tilde{F}_z$ in (96) vanish. We choose to cancel F_z, implying that we decouple the vertical-linear motion from the vertical-angular motion. That is accomplished if

$$\frac{k^1_{p,z}}{k^2_{p,z}} = \frac{k^1_{d,z}}{k^2_{d,z}} = \frac{k^1_{i,z}}{k^2_{i,z}} = \frac{-m_2 d_2 (J + d_1 m_1 (d_1 - d_2))}{+m_1 d_1 (J + d_2 m_2 (d_2 - d_1))} =: \frac{\Delta_{z,1}}{\Delta_{z,2}}. \tag{97}$$

That is, the proportional, derivative and integral gains of each vehicle must respect a ratio, which is exactly 1 under symmetry conditions (see (73)). In order to satisfy the conditions above, let, for $h \in \{p, i, d\}$,

$$k^1_{h,z} = \frac{2\Delta_{z,1}}{\Delta_{z,1} + \Delta_{z,2}} k_{h,z}, k^2_{h,z} = \frac{2\Delta_{z,2}}{\Delta_{z,1} + \Delta_{z,2}} k_{h,z}, \tag{98}$$

for some positive $k_{p,z}$, $k_{i,z}$, and $k_{d,z}$. If the vehicles' gains are chosen as in (98), then

$$A_{z,\theta} = \begin{bmatrix} A_z & 0_{3\times 3} \\ \star_{3\times 3} & A_\theta \end{bmatrix} \in \mathbb{R}^{(3+3)\times(3+3)} \tag{99a}$$

where (recall C_3 in (55))

$$A_z = C_3\left(\gamma_z(k_{i,z}, k_{p,z}, k_{d,z})\right), \tag{99b}$$

$$A_\theta = C_3\left(\gamma_\theta(k_{i,z}, k_{p,z}, k_{d,z})\right), \tag{99c}$$

and where

$$\gamma_\theta = \left(1 + \frac{J(d_1 m_1 - d_2 m_2)}{2(-d_1 d_2) m_1 m_2 (d_1 - d_2)}\right)^{-1} > 0, \tag{99d}$$

$$\gamma_z = \gamma_\theta \frac{\Delta_{z,1}\Delta_{z,2}}{(d_1 d_2 (d_1 - d_2) m_1 m_2)^2} \left(1 + \frac{m(d_1^2 m_1 + d_2^2 m_2) + J(m + m_1 + m_2)}{(d_1 - d_2)^2 m_1 m_2}\right)^{-1} > 0. \tag{99e}$$

It follows from (55) that A_z and A_θ are Hurwitz (and therefore also $A_{z,\theta}$), provided that

$$k_{i,z} < \min(\gamma_z, \gamma_\theta) k_{p,z} k_{d,z}. \tag{100}$$

i.e., provided that the integral gain is *small enough*. Note that, for a regular PID, it is required that $k_{i,z} < k_{p,z}k_{d,z}$, while the constraint above is more restrictive, since $\gamma_\theta < 1$. Moreover, notice that γ_θ vanishes when either d_1 or d_2 vanish (the distance of the contact points to the bar's center-of-mass): as such, it is advisable to have *large* $|d_1|$ and $|d_2|$ (*large* in the sense that $\frac{J(d_1 m_1 - d_2 m_2)}{(-d_1 d_2) m_1 m_2 (d_1 - d_2)} \ll 1$), because γ_θ is closer to 1 (and thus the bound on the integral gain is less restrictive). This also agrees with intuition, which suggests that controlling the bar's attitude when the contact points are *too close* to the bar's center-of-mass is difficult.

Remark 27: The coefficients γ_z and γ_θ in (99e) and (99d) are positive since d_1 and d_2 have opposite signs.

Remark 28: The attitude gains of the vehicles do not play a role in the linearized vertical motion.

We can now present our main result.

Theorem 29: Consider the UAVs-bar system, with vector field in (30), the dynamic control law (48) whose internal (integral) states evolve as in (40b), and the resulting closed-loop vector field $\tilde{Z}^{cl}_\gamma$ in (52). Consider also the equilibrium $\tilde{z}^{cl}_\gamma$ in (44), and let the desired configuration be $\gamma = \gamma_\star$ with $\theta_\star = 0$ and $F_\star = 0$ (i.e., the bar is to be stabilized on the horizontal plane and under no normal stress). Let also d_1 and d_2 have opposite signs. Finally, let the longitudinal, lateral and vertical gains of the

control laws be chosen as in (85), (92) and (97), respectively, and such that (i) the attitude gain is big enough, as quantified in (88) and (94); and such that (ii) the integral gain is small enough, as quantified in (100). It then follows that the equilibrium $\tilde{z}_\gamma^{cl}$ is exponentially stable.

Our main result, in Theorem 29, states that pose stabilization of the bar is accomplished, provided that the UAVs-bar system starts in some neighborhood of the equilibrium. The experiments provided in [31], [32] provide insight into the region of attraction of the equilibrium; in particular, convergence to the equilibrium was verified after impulsive disturbances were applied on both the bar and the UAVs.

E. Bar with non-zero pitch

In this section, we study the effect of requiring the angular position of the bar to have a non-zero vertical component (non-zero pitch angle), i.e.,

$$\gamma_\star := (p_\star, n_\star, F_\star) \text{ with } p_\star := (0,0,0), n_\star := (|\cos(\theta_\star)|, 0, \sin(\theta_\star)) \text{ and } F_\star := 0, \tag{101}$$

with $\theta_\star \in \left(-\frac{\pi}{2}, \frac{\pi}{2}\right)$. This equilibrium configuration corresponds to the bottom left configuration shown in Fig. 3. For this purpose, and for simplicity, we assume that the UAVs are fully-actuated, that the system is symmetric (as defined in (73)), and that no integral action is being used. Let us anticipate the results that follow, where we find out that the vertical angular motion is coupled with the longitudinal angular motion.

For this system, a Jacobian $A \in \mathbb{R}^{24\times 24}$ is computed[13], and the following similarity matrix is used,

$$P := \begin{bmatrix} P_z & P_{\theta,\delta} & P_x & P_y & P_\psi & P_\perp \end{bmatrix}^T \in \mathbb{R}^{24\times 24}, \tag{102a}$$

where (below $e_1, \cdots, e_{24}$ are the canonical basis vectors in $\mathbb{R}^{24}$)

$$P_z := \begin{bmatrix} e_3 & Ae_3 \end{bmatrix} \in \mathbb{R}^{24\times 2}, \tag{102b}$$

$$P_{\theta,\delta} := \begin{bmatrix} e_6 & Ae_6 & \nu & A\nu \end{bmatrix}|_{\nu = e_7 - e_{10}} \in \mathbb{R}^{24\times 4}, \tag{102c}$$

$$P_x := \begin{bmatrix} e_1 & Ae_1 & A^2e_1 & A^3e_1 \end{bmatrix} \in \mathbb{R}^{24\times 4}, \tag{102d}$$

$$P_y := \begin{bmatrix} e_2 & Ae_2 & A^2e_2 & A^3e_2 \end{bmatrix} \in \mathbb{R}^{24\times 4}, \tag{102e}$$

$$P_\psi := \begin{bmatrix} e_5 & Ae_5 & A^2e_5 & A^3e_5 \end{bmatrix} \in \mathbb{R}^{24\times 4}, \tag{102f}$$

and whose determinant $|P| = -\frac{2d^2 g^6 m^2 \cos^2(\theta_\star)}{J^2 L^{10}}$ is non-zero since $\theta_\star \in \left(-\frac{\pi}{2}, \frac{\pi}{2}\right)$ (and where $P_\perp := (Df(z_\gamma))^T \in \mathbb{R}^{24\times 6}$ with f as defined in (5)). Given the state matrix A and the change of basis matrix P in (102a), it then follows that

$$PAP^{-1} = \begin{bmatrix} A_z \oplus A_{\theta,\delta} \oplus A_x \oplus A_y \oplus A_\psi & \star \\ 0_{6\times 24} & -\lambda I_{6\times 6} \end{bmatrix} \in \mathbb{R}^{24\times 24}, \tag{103a}$$

where

$$A_z = C_2(\gamma_z(k_{p,z}, k_{d,z}))|_{\gamma_z = \left(1+\frac{m}{2M}\right)^{-1}}, \tag{103b}$$

$$A_x = \Gamma_4\left(q, f_p, k\right)|_{q=\frac{m}{2M}, f_p = \frac{g}{l}, k=(k_{p,x}, k_{d,x})}, \tag{103c}$$

$$A_y = \Gamma_4\left(q, f_p, k\right)|_{q=\frac{m}{2M}, f_p = \frac{g}{l}, k=(k_{p,y}, k_{d,y})}, \tag{103d}$$

$$A_\psi = \Gamma_4\left(q, f_p, k\right)|_{q=\frac{J}{d^2 m}\frac{m}{2M}, f_p = \frac{d^2 m}{J}\frac{g}{l}, k=(k_{p,y}, k_{d,y})}, \tag{103e}$$

which are all Hurwitz; and where

$$A_{\theta,\delta} = \begin{bmatrix} C_2\left(-\gamma_\theta\left(k_{p,z} + \tan(\theta_\star)^2 f_{p,x}, k_{d,z}\right)\right) & -\frac{f_{p,x}}{2d}\gamma_\theta \tan(\theta_\star) e_2 e_1^T \\ -2d\tan(\theta_\star) f_{p,x} e_2 e_1^T & C_2\left(-\left(k_{p,x} + f_{p,x}, k_{d,x}\right)\right) \end{bmatrix}|_{\substack{\gamma_\theta = \left(1+\frac{J}{d^2 m}\frac{m}{2M}\frac{1}{\cos(\theta_\star)^2}\right)^{-1} \\ f_{p,x} = \frac{g}{l}\frac{m}{2M}}} \in \mathbb{R}^{(2+2)\times(2\times 2)}, \tag{103f}$$

which is Hurwitz for all $\theta_\star \in \left(-\frac{\pi}{2}, \frac{\pi}{2}\right)$. It follows from (103a) that the vertical linear, the longitudinal linear, the lateral linear and the lateral angular motions are all decoupled. On the other hand, it follows from (103f) that the vertical angular motion is coupled to the longitudinal angular motion when $\theta_\star \neq 0$. This coupling is, nonetheless, not detrimental to the stability of the equilibrium configuration, as the matrix $A_{\theta,\delta}$ is Hurwitz for all $\theta_\star \in \left(-\frac{\pi}{2}, \frac{\pi}{2}\right)$. However, this conclusion is only valid for fully actuated UAVs; for under-actuated UAVs or for UAVs with vertical integral action, stricter conditions on the allowed interval for $\theta_\star$ may be required.

[13] $A = DZ_\gamma^{cl}(z_\gamma)$ where $Z_\gamma^{cl}(z) := Z(z, u_\gamma^{pd}(z))$, with Z in (8b), z_γ in (23) and u_γ^{pd} in (36).

F. Bar under non-zero normal force

In this section, we study the effect of requiring the bar to be under a non-zero normal stress/force, i.e.,

$$\gamma_\star := (p_\star, n_\star, F_\star) \text{ with } p_\star := (0,0,0), n_\star := (1,0,0) \text{ and } F_\star := r\frac{mg}{2}, \tag{104}$$

for some $r \in \mathbb{R}$. This equilibrium configuration corresponds to the top right configurations shown in Fig. 3. Recall that $F_\star$ is twice the normal stress exerted on the bar and, for that reason, r represents the ratio of the normal force exerted on the bar with respect the the bar's weight. In studying this scenario, and for simplicity, we assume that the UAVs are fully-actuated, that the system is symmetric (as defined in (73)), and that no integral action is being used. Let us anticipate the results that follow, where we find out that the vertical and longitudinal motions are coupled, and that requiring the bar to be under tension is more beneficial than requiring the bar to be under compression.

For this system, a Jacobian $A \in \mathbb{R}^{24\times 24}$ is computed[14], and the following similarity matrix is used,

$$P := \begin{bmatrix} P_{z,\delta} & P_{p,\theta} & P_y & P_\psi & P_\perp \end{bmatrix}^T \in \mathbb{R}^{24\times 24}, \tag{105a}$$

where (below $e_1, \cdots, e_{24}$ are the canonical basis vectors in $\mathbb{R}^{24}$)

$$P_{z,\delta} := \begin{bmatrix} e_3 & Ae_3 & \nu & A\nu \end{bmatrix}|_{\nu = e_7 - e_{10}} \in \mathbb{R}^{24\times 4}, \tag{105b}$$

$$P_{p,\theta} := \begin{bmatrix} p & Ap & A^2p & A^3p & e_6 & Ae_6 \end{bmatrix}|_{p = e_1 - d\frac{J}{d^2 m} r e_6} \in \mathbb{R}^{24\times 6}, \tag{105c}$$

$$P_y := \begin{bmatrix} e_2 & Ae_2 & A^2e_2 & A^3e_2 \end{bmatrix} \in \mathbb{R}^{24\times 4}, \tag{105d}$$

$$P_\psi := \begin{bmatrix} e_5 & Ae_5 & A^2e_5 & A^3e_5 \end{bmatrix} \in \mathbb{R}^{24\times 4}, \tag{105e}$$

and whose determinant $|P| = -\frac{2d^2 g^6 m^2 (1+r^2)^3}{J^2 L^{10}}$ is non-zero for any $r \in \mathbb{R}$ (and where $P_\perp := (Df(z_\gamma))^T \in \mathbb{R}^{24\times 6}$ with f as defined in (5)). The point $p = e_1 - d\frac{J}{d^2 m} r e_6$ in (105c) is special in the sense that its position, velocity, acceleration and jerk (i.e., A^0p, A^1p, A^2p and A^3p) do not depend on any controller gains; this in turn guarantees that the change of basis matrix P also does not depend on any controller gains[15]. Given the state matrix A and the change of basis matrix P in (105a), it then follows that

$$PAP^{-1} = \begin{bmatrix} A_{z,\delta} \oplus A_{p,\theta} \oplus A_y \oplus A_\psi & \star \\ 0_{6\times 24} & -\lambda I_{6\times 6} \end{bmatrix} \in \mathbb{R}^{24\times 24}, \tag{106a}$$

where

$$A_{z,\delta} = \left(C_2 \left(-\gamma_z \left(k_{p,z}, k_{d,z} \right) \right)|_{\gamma_z = \left(1+\frac{m}{2M}\right)^{-1}} \right) \oplus \left(C_2 \left(-\left(k_{p,x} + f_{p,x}, k_{d,x} \right) \right)|_{f_{p,x} = \frac{g}{l}\frac{m}{2M}} \right) + \mathcal{O}(|r|) \in \mathbb{R}^{4\times 4}, \tag{106b}$$

$$A_{p,\theta} = \left(\Gamma_4 \left(q_x, f_{p,x}, k \right)|_{q_x = \frac{m}{2M}, f_{p,x} = \frac{g}{l}, k = (k_{p,x}, k_{d,x})} \right) \oplus \left(C_2 \left(-\gamma_\theta \left(k_{p,z}, k_{d,z} \right) \right)|_{\gamma_\theta = \left(1+\frac{J}{d^2 m}\frac{m}{2M}\right)^{-1}} \right) + \mathcal{O}(|r|) \in \mathbb{R}^{6\times 6}, \tag{106c}$$

$$A_y = \Gamma_4 \left(q_y, f_{p,y}, k \right)|_{q_y = \frac{m}{2M}, f_{p,y} = \frac{g}{l}\sqrt{1+r^2}, k = (k_{p,y}, k_{d,y})}, \tag{106d}$$

$$A_\psi = \tilde{\Gamma}_4 \left(\tilde{q}_\psi, q_\psi, f_{p,\psi}, k \right)|_{\tilde{q}_\psi = \frac{\delta - 1}{\delta}, q_\psi = \frac{J}{d^2 m}\frac{q_y}{\delta}, f_{p,\psi} = \frac{d^2 m}{J}\delta f_{p,y}, k = (k_{p,y}, k_{d,y})}|_{\delta = 1 + \frac{l}{d}\frac{r}{\sqrt{1+r^2}}}. \tag{106e}$$

It follows from above that, when the bar is under a non-zero normal force, the linear vertical motion is coupled with the angular longitudinal motion (where the coupling vanishes when $r = 0$); the motion of the position p (which corresponds to the linear longitudinal motion when $r = 0$) is coupled with the angular vertical motion (where the coupling vanishes when $r = 0$); where the only influence of the normal force in the linear lateral motion is to increase the frequency $f_{p,y}$ (A_y in (106d) is Hurwitz regardless of r); and, finally, where the lateral angular motion is significantly influenced by the normal force, i.e., A_ψ in (106e) is Hurwitz only if (note that $q_\psi(1 - \tilde{q}_\psi) = \frac{J}{d^2 m}\frac{m}{2M}\delta^{-2} > 0$, as required by (58c))

$$k_{p,y} > -f_{p,\psi} q_\psi \tilde{q}_\psi = -\frac{g}{l}\frac{m}{2M}\frac{r}{\frac{d}{l} + \frac{r}{\sqrt{1+r^2}}}. \tag{107}$$

This result confirms our intuition (next, and w.l.o.g., we assume that $d > 0$). For simplicity, let $d > l$. Then, when we want the bar to be under tension ($r > 0$), it suffices for the proportional gain $k_{p,y}$ to be positive; on the other hand, when we want the bar to be under compression ($r < 0$), the proportional gain $k_{p,y}$ needs to be strictly positive (and arbitrarily large, if $|r|$ is arbitrarily large). As such, one can say that requiring the bar to be under compression is less stable than requiring the bar to be under tension, because a bar under tension tends to restore the yaw position of the bar, while a bar under compression tends to destabilize the yaw position of the bar. This conclusion confirms the comments drawn during the analysis of the open-loop equilibria (see discussion after Proposition 4).

Remark 30: If $d < l$ then the UAVs can cross paths, and there are three scenarios: when we want the bar to be under tension ($r > 0$), it suffices for the proportional gain $k_{p,y}$ to be positive; when we want the bar to be under *mild* compression

[14] $A = DZ_\gamma^{cl}(z_\gamma)$ where $Z_\gamma^{cl}(z) := Z(z, u_\gamma^{pd}(z))$, with Z in (8b), z_γ in (23) and u_γ^{pd} in (36).

[15] In particular, when $r = 0$, then $p = e_1$ which corresponds to the longitudinal linear position of the bar.

($-\frac{d}{\sqrt{l^2-d^2}} < r < 0$), the proportional gain $k_{p,y}$ needs to be strictly positive, and infinitely large as r approaches $-\frac{d}{\sqrt{l^2-d^2}}$ (when $r = -\frac{d}{\sqrt{l^2-d^2}}$, then $p_{1,\gamma} = p_{2,\gamma}$, which corresponds to a scenario where the UAVs overlap); finally, when we want the bar to be under *strong* compression ($r < -\frac{d}{\sqrt{l^2-d^2}}$), then, once again, it suffices that the proportional gain $k_{p,y}$ be positive.

Remark 31: Notice that $A_{z,\delta}$ and $A_{p,\theta}$ are Hurwitz when $r = 0$, and, by continuity of the eigenvalues of a matrix, we can conclude that there is a neighborhood around 0, such that those matrices remain Hurwitz when r is in that neighborhood (that is, for a bar under some *small* tension or *small* compression, the matrices remain Hurwitz).

VII. Experimental Results

We experimented the proposed control laws for a symmetric system and for a non-symmetric system. The symmetric system is that illustrated in Fig. 1a, and the non-symmetric system is that illustrated in Fig. 1b. A video of the experiments is found at https://youtu.be/ywwPvZuVpF0 and at https://youtu.be/rgweowQ8fAE, and a detailed description of the corresponding experimental results is found in [31] and [32].

VIII. Conclusions

We proposed a control law for pose stabilization of a bar-cargo tethered to two UAVs. We modeled the system via a Newtonian approach, where we exploited the fact that the cables, connecting the bar to the UAVs, constrain the motion of the system to a manifold. We closed the loop with a saturated PID-like control law, for which one can guarantee that physical input limitations of each UAV are respected. Finally, we provided conditions on the PID gains that guarantee that pose stabilization is accomplished; we described good and bad types of asymmetries; and we inferred that requiring the bar-cargo to be under tension is better for stability, as opposed to requiring the bar-cargo to be under compression.

References

[1] AEROWORKS aim. http://www.aeroworks2020.eu/. (accessed April, 2018).

[2] Q. Jiang and V. Kumar. The inverse kinematics of cooperative transport with multiple aerial robots. *IEEE Transactions on Robotics*, 29(1):136–145, Feb 2013.

[3] M. Tognon, S. S. Dash, and A. Franchi. Observer-based control of position and tension for an aerial robot tethered to a moving platform. *IEEE Robotics and Automation Letters*, 1(2):732–737, July 2016.

[4] Marco M. Nicotra, Roberto Naldi, and Emanuele Garone. Nonlinear control of a tethered UAV: The taut cable case. *Automatica*, 78:174 – 184, 2017.

[5] G. Schmidt and R. Swik. Automatic hover control of an unmanned tethered rotorplatform. *Automatica*, 10(4):393 – 403, 1974.

[6] P. E. I. Pounds and A. M. Dollar. Stability of helicopters in compliant contact under PD-PID control. *IEEE Transactions on Robotics*, 30(6):1472–1486, Dec 2014.

[7] P. J. Cruz, M. Oishi, and R. Fierro. Lift of a cable-suspended load by a quadrotor: A hybrid system approach. In *American Control Conference*, pages 1887–1892, July 2015.

[8] Lorenzo Marconi, Roberto Naldi, and Luca Gentili. Modelling and control of a flying robot interacting with the environment. *Automatica*, 47(12):2571 – 2583, 2011.

[9] A. Suarez, G. Heredia, and A. Ollero. Lightweight compliant arm with compliant finger for aerial manipulation and inspection. In *IEEE/RSJ International Conference on Intelligent Robots and Systems*, pages 4449–4454, Oct 2016.

[10] C. Korpela, M. Orsag, M. Pekala, and P. Oh. Dynamic stability of a mobile manipulating unmanned aerial vehicle. In *International Conference on Robotics and Automation*, pages 4922–4927, 2013.

[11] Hai-Nguyen Nguyen, ChangSu Ha, and Dongjun Lee. Mechanics, control and internal dynamics of quadrotor tool operation. *Automatica*, 61:289 – 301, 2015.

[12] I. Palunko, P. Cruz, and R. Fierro. Agile load transportation: Safe and efficient load manipulation with aerial robots. *IEEE Robotics Automation Magazine*, 19(3):69–79, Sept 2012.

[13] S. Tang and V. Kumar. Mixed integer quadratic program trajectory generation for a quadrotor with a cable-suspended payload. In *IEEE International Conference on Robotics and Automation*, pages 2216–2222, May 2015.

[14] M. Tognon and A. Franchi. Dynamics, control, and estimation for aerial robots tethered by cables or bars. *IEEE Transactions on Robotics*, 33(4):834–845, Aug 2017.

[15] S. J. Lee and H. J. Kim. Autonomous swing-angle estimation for stable slung-load flight of multi-rotor UAVs. In *IEEE International Conference on Robotics and Automation*, pages 4576–4581, May 2017.

[16] Morten Bisgaard, Anders la Cour-Harbo, and Jan Dimon Bendtsen. Adaptive control system for autonomous helicopter slung load operations. *Control Engineering Practice*, 18(7):800 – 811, 2010. Special Issue on Aerial Robotics.

[17] Shicong Dai, Taeyoung Lee, and Dennis S Bernstein. Adaptive control of a quadrotor UAV transporting a cable-suspended load with unknown mass. In *IEEE 53rd Annual Conference on Decision and Control*, pages 6149–6154. IEEE, 2014.

[18] F. A. Goodarzi and T. Lee. Dynamics and control of quadrotor UAVs transporting a rigid body connected via flexible cables. In *American Control Conference*, pages 4677–4682, July 2015.

[19] T. Lee, K. Sreenath, and V. Kumar. Geometric control of cooperating multiple quadrotor UAVs with a suspended payload. In *IEEE 52nd Annual Conference on Decision and Control*, pages 5510–5515, Dec 2013.

[20] Konstantin Kondak, Markus Bernard, Fernando Caballero, Ivan Maza, and Anibal Ollero. Cooperative autonomous helicopters for load transportation and environment perception. *Advances in Robotics Research*, pages 299–310, 2009.

[21] P. O. Pereira and D. V. Dimarogonas. Control framework for slung load transportation with two aerial vehicles. In *IEEE 56th Annual Conference on Decision and Control*, pages 4254–4259, Dec 2017.

[22] T. Lee. Collision avoidance for quadrotor UAVs transporting a payload via voronoi tessellation. In *American Control Conference*, pages 1842–1848, July 2015.

[23] P. O. Pereira and D. V. Dimarogonas. Nonlinear pose tracking controller for bar tethered to two aerial vehicles with bounded linear and angular accelerations. In *IEEE 56th Annual Conference on Decision and Control*, pages 4260–4265, Dec 2017.

[24] T. Lee. Geometric control of multiple quadrotor UAVs transporting a cable-suspended rigid body. In *IEEE 53rd Annual Conference on Decision and Control*, pages 6155–6160, 2014.

[25] Nathan Michael, Jonathan Fink, and Vijay Kumar. Cooperative manipulation and transportation with aerial robots. *Autonomous Robots*, 30(1):73–86, 2011.

[26] M. Gassner, T. Cieslewski, and D. Scaramuzza. Dynamic collaboration without communication: Vision-based cable-suspended load transport with two quadrotors. In *IEEE International Conference on Robotics and Automation*, pages 5196–5202, May 2017.

[27] H. Lee, H. Kim, and H. J. Kim. Planning and control for collision-free cooperative aerial transportation. *IEEE Transactions on Automation Science and Engineering*, PP(99):1–13, 2017.

[28] S. Kim, S. Choi, H. Lee, and H. J. Kim. Vision-based collaborative lifting using quadrotor UAVs. In *14th International Conference on Control, Automation and Systems*, pages 1169–1174, Oct 2014.

[29] M. Mohammadi, A. Franchi, D. Barcelli, and D. Prattichizzo. Cooperative aerial tele-manipulation with haptic feedback. In *IEEE/RSJ International Conference on Intelligent Robots and Systems*, pages 5092–5098, Oct 2016.

[30] C. Masone, H. H. Bülthoff, and P. Stegagno. Cooperative transportation of a payload using quadrotors: A reconfigurable cable-driven parallel robot. In *IEEE/RSJ International Conference on Intelligent Robots and Systems*, pages 1623–1630, Oct 2016.

[31] P. O. Pereira and D. V. Dimarogonas. Collaborative transportation of a bar by two aerial vehicles with attitude inner loop and experimental validation. In *IEEE 56th Annual Conference on Decision and Control*, pages 1815–1820, Dec 2017.

[32] P. O. Pereira, P. Roque, and D. V. Dimarogonas. Asymmetric collaborative bar stabilization tethered to two heterogeneous aerial vehicles. In *2018 IEEE International Conference on Robotics and Automation*, 2018 (to appear).

[33] A. Tagliabue, M. Kamel, S. Verling, R. Siegwart, and J. Nieto. Collaborative transportation using MAVs via passive force control. In *IEEE International Conference on Robotics and Automation*, pages 5766–5773, May 2017.

[34] P. O. Pereira and D. V. Dimarogonas. Stability of load lifting by a quadrotor under attitude control delay. In *IEEE International Conference on Robotics and Automation*, pages 3287–3292, May 2017.

[35] M. Orsag, C. Korpela, M. Pekala, and P. Oh. Stability control in aerial manipulation. In *American Control Conference*, pages 5581–5586, June 2013.

[36] Jorge Cortés Monforte. *Geometric Control and Numerical Aspects of Nonholonomic Systems*. Springer-Verlag, 2002.

[37] R. C. Nelson. *Flight Stability and Automatic Control*, volume 2. WCB/McGraw Hill, 1998.